TÜBİTAK

Turkish Journal of Earth Sciences

http://journals.tubitak.gov.tr/earth/

Research Article

Turkish J Earth Sci
(2013) 22: 891-918

doi:10.3906/yer-1207-8

Circum-Tethyan carbonate platform evolution during the Palaeogene: the Prebetic platform as a test for climatically controlled facies shifts

Stefan HÖNTZSCH[1], Christian SCHEIBNER[2,*], Johannes P. BROCK[2], Jochen KUSS[2]
[1]K + S, Kassel, Germany
[2]Department of Geosciences, Bremen University, Bremen, Germany

Received: 18.07.2012 • **Accepted:** 16.06.2013 • **Published Online:** 11.10.2013 • **Printed:** 08.11.2013

Abstract: The distribution of selected shallow-benthic biota at circum-Tethyan carbonate platforms demonstrates an excellent proxy for the impact of latitudinally controlled cooling and variations in the trophic resources during the Palaeogene. In this study, we link and compare the spatial distribution and abundance of larger benthic foraminifera and hermatypic corals of Tethyan carbonate successions with new records from the Prebetic platform in SE Spain. The succession of the Prebetic platform is dominated by larger benthic foraminifera and coralline red algae throughout the Eocene, whereas corals were not recorded until the Late Eocene. Similar biotic trends were reported from 10 selected circum-Tethyan carbonate platforms. High-resolution carbon isotopes indicate a decoupling from the global carbon cycle during the latest Eocene and Early Oligocene. Thus, a possible scenario is demonstrated by the increasing restriction of the Prebetic shelf due to the continuing convergence of the Betic domain towards Iberia during the Early Oligocene. Based on previous studies, we refined earlier established Palaeogene platform stages, which reflect the evolution of shallow-benthic communities during the transition from global greenhouse to icehouse conditions. Global cooling led to the recovery of coral communities in the northern Tethyan realm during the Bartonian (stage IV). A prominent cooling event at the Bartonian–Priabonian boundary, associated with the demise of many symbiont-bearing larger foraminifera, caused the proliferation of coral reefs in the northern Tethys and the recovery of corals in the southern Tethys (stage V). The massive temperature drop related to the Oi-1 glaciation represented the base of platform stage VI (Early Oligocene–?). After a transient platform crisis during the lowermost Oligocene, coral reefs spread throughout the Tethys and proliferated with newly emerged larger benthic foraminifera.

Key words: Prebetic platform, Palaeogene platform stages, Tethys, larger benthic foraminifera, coral reefs, carbon isotopes, palaeoclimate, Spain

1. Introduction

Carbonate platform systems represent an excellent example of ancient sediment archives, which provide crucial data regarding the reconstruction of continental margins. Platform evolution is influenced and controlled by multiple processes, including global and regional climate variability, global and local tectonics, eustatic sea level variations, and the changing dominance of platform biota through time. The interactions of those processes create highly dynamic and complex environmental scenarios. One main problem regarding the reconstruction of shallow marine inner platform settings is the frequent subaerial exposure during sea level lowstands, causing erosion, karstification, and major hiati at the platform. To understand the evolution and the dynamics of carbonate platforms, mass flow deposits at the platform slope represent an excellent tool for the reconstruction of those systems. In contrast to the shallow marine platform interior, mass flow deposits at the outer neritic and bathyal slope are less altered and better preserved. Their biotic compositions and geochemical signatures record environmental shifts from the remote platform interior, especially during times of climatic and tectonic instability.

The Palaeogene represents an epoch in Earth's history that is characterised by high climatic variability and the reorganisation of major continental plates in the Mediterranean realm. The transition from the Early Cenozoic greenhouse to the Late Cenozoic icehouse, punctuated by multiple climatic perturbations, is recorded by various environmental parameters and organisms at the marginal shelves (e.g., climatically controlled facies shifts, shifts in the trophic regime, and varying carbon isotope signatures). Furthermore, the continuing convergence of the African Craton and Eurasia, leading to the reactivation and progradation of ancient fault systems, causes major incisions in the marginal marine environments in the Tethyan realm. Studying the impact of those perturbations on carbonate platforms will help to understand the

* Correspondence: scheibne@uni-bremen.de

dynamics of depositional processes at passive continental margins.

An excellent example for such a highly dynamic environment is represented by the South Iberian continental margin in the NW Tethys during the Palaeogene. The stratigraphic record of this passive margin reveals a complex framework of autochthonous and allochthonous units, which have been deformed during multiple phases of tectonic activity, culminating during the Miocene uplift of the Betic Cordillera. The pre-orogenic sedimentary record of the passive South Iberian margin contains a heterogeneous suite of slope-related hemipelagites and shallow marine platform carbonates. This succession has been studied intensively with respect to the tectono-stratigraphic evolution of the Betic domain since the Mesozoic. Various local studies reveal facies patterns and depositional processes, especially of the undisturbed marly successions of the deeper shelf. However, a coherent model of a detached carbonate platform regarding the fundamental biotic evolution during times of high climatic and tectonic variability is missing. In this study we link and compare the data of 10 circum-Tethyan carbonate platforms with the succession of the South Iberian margin to achieve new information regarding timing and biotic impact of the Early Palaeogene greenhouse to Late Palaeogene icehouse transition. We conducted a high resolution microfacies analysis comparable to the study of Hoentzsch *et al.* (2011a) of proximal and distal mass flow deposits, as well as creating a new carbon isotope record of these deposits. These results will reveal the impact of long- and short-term climatic evolution to shallow marine benthic assemblages, especially to larger benthic foraminifera and corals.

1.1. Climatic evolution during the Palaeogene

The Palaeogene is known as a period in Earth's history that underwent fundamental long-term and transient climatic changes, resulting in the transition from global greenhouse to icehouse conditions (Zachos *et al.* 2001). The Early Palaeogene (Palaeocene–Middle Eocene) is characterised by global greenhouse conditions, culminating during the Early Eocene Climatic Optimum between 53 and 49 Ma (Figure 1). Anomalous warm poles and low latitudinal temperature gradients caused strongly decreased ocean circulations with highly oligotrophic open ocean conditions (Hallock *et al.* 1991; Gibbs *et al.* 2006). This Early Palaeogene "hothouse" was, however, superimposed by multiple transient climatic perturbations, which are attributed to significant negative shifts in the global carbon cycle ("hyperthermals" or Eocene thermal maxima; Thomas & Zachos 2000; Cramer *et al.* 2003; Lourens *et al.* 2005). The most prominent carbon cycle perturbation is the Palaeocene–Eocene Thermal Maximum, resulting in a global transient temperature increase of 4–8 °C and major environmental turnover in nearly all environments on Earth (e.g., Kennett & Stott 1991; Beerling 2000; Bowen *et al.* 2004).

The post-Early Eocene Climatic Optimum climate is characterised by a cooling of higher latitudes, whereas the tropics remained warm (Pearson *et al.* 2007). The increasing latitudinal temperature gradients strengthened global oceanic currents, causing the upwelling of cooler deep ocean waters and the eutrophication of the oceans (Hallock *et al.* 1991). The temperature decline during the Middle and Late Eocene was interrupted by the Middle Eocene Climatic Optimum between ~41.5 and 40 Ma, affecting both surface and bathyal environments (Figure 1; Bohaty & Zachos 2003; Bijl *et al.* 2010). However, this transient warming was not affected by a significant negative carbon isotope excursion (Jovane *et al.* 2007). The continuing cooling in the second half of the Eocene led to the occurrence of the first ephemeral Antarctic ice sheets in the second half of the Eocene. A major break in global climate since the end of the Early Eocene Climatic Optimum is represented by the Oi-1 glaciation at ~34 Ma, coinciding with the Eocene–Oligocene boundary (Figure 1; Zachos *et al.* 2001, 2008; DeConto *et al.* 2008). A sharp global temperature drop is associated with a positive carbon isotope excursion of ~1‰ and a major biotic reorganisation (Ivany *et al.* 2000; Zanazzi *et al.* 2007; Eldrett *et al.* 2009). The Oi-1 glaciation demonstrates the onset of permanent Antarctic ice sheets and a strong demise in global carbonate platform systems. Thus, the Eocene–Oligocene boundary represents the final transition from climatic optimum conditions to icehouse conditions.

1.2. Concepts on biotic shifts during Palaeogene platform evolution

The evolution of carbonate platform systems during the Palaeogene was strongly influenced by long-term global climatic and tectonic turnover and transient perturbations. The spatial and quantitative distribution of platform-building organisms through time shows a clear connection to the environmental turnover in the Palaeogene (Hallock *et al.* 1991; McGowran & Li 2001; Nebelsick *et al.* 2005). The timing and biotic effects of environmental transitions during the Palaeogene were raised in multiple biosedimentary concepts. Hallock *et al.* (1991) presented the first compilation of Palaeogene evolutionary events for larger benthic foraminifera and planktic foraminifera with respect to the effects of varying trophic resources in the oceans (trophic resource continuum). Hottinger (1997, 1998) and McGowran and Li (2001) link the evolution of Tethyan larger foraminifera to major changes in climate and define the major Cenozoic larger benthic foraminifera assemblages as chronofaunas. Brasier (1995) and Hottinger (2001) introduce the concept of global community maturation cycles for larger benthic

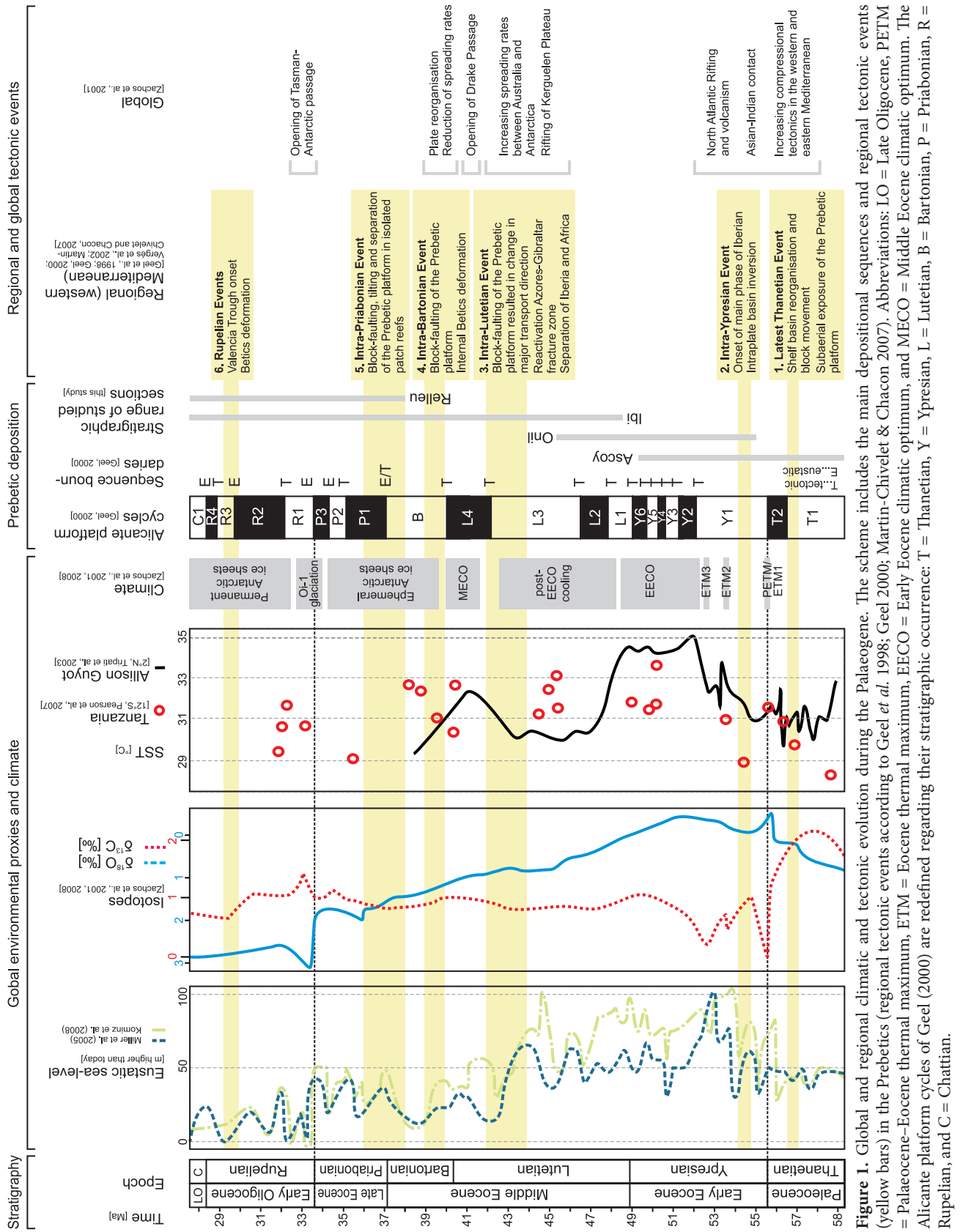

Figure 1. Global and regional climatic and tectonic evolution during the Palaeogene. The scheme includes the main depositional sequences and regional tectonic events (yellow bars) in the Prebetics (regional tectonic events according to Geel *et al.* 1998; Geel 2000; Martín-Chivelet & Chacón 2007). Abbreviations: LO = Late Oligocene, PETM = Palaeocene–Eocene thermal maximum, ETM = Eocene thermal maximum, EECO = Early Eocene climatic optimum, and MECO = Middle Eocene climatic optimum. The Alicante platform cycles of Geel (2000) are redefined regarding their stratigraphic occurrence: T = Thanetian, Y = Ypresian, L = Lutetian, B = Bartonian, P = Priabonian, R = Rupelian, and C = Chattian.

foraminifera. According to this approach, larger benthic foraminifera evolution can be classified into 4 (Brasier) or 5 (Hottinger) phases of increasing habitat adaptation and improving life strategies. Both authors suggest that each global community maturation cycle is terminated by a mass extinction.

The described concepts have been applied to selected critical intervals during the Palaeogene. Scheibner and Speijer (2008a) show that the global warming during the early Palaeogene caused a Tethyan-wide massive decline in coral reefs and a coeval shift to larger carbonate platforms dominated by benthic foraminifera. The authors define the circum-Tethyan platform stages and link the evolutionary impact of the larger foraminifera turnover (Orue-Etxebarria *et al*. 2001) at the Palaeocene–Eocene boundary directly to the Palaeocene–Eocene thermal maximum. Nebelsick *et al*. (2005) summarise changes in specific carbonate facies types in the circum-alpine area during the Middle Eocene to Oligocene and introduce the concept of facies dynamics. The authors argue that major carbonate platform organisms are controlled by phylogenetic, ecological, and geological parameters. The following paragraphs summarise the main steps in Palaeogene carbonate platform evolution with respect to the introduced concepts.

1.2.1. Palaeocene

The global ocean crisis during the Cretaceous–Palaeogene transition at 65.5 Ma led to a massive specific decline in global shallow benthic assemblages. A long-term sea level rise during the Early Palaeocene created new shelf areas and vacant biological niches (Buxton & Pedley 1989). The created vacant niches were occupied by larger benthic foraminifera and corals, which became a major part of shallow benthic assemblages (first phase of the global community maturation cycle; Hottinger 2001). At around 60 Ma, new larger benthic foraminifera with complex morphologies appeared (second phase of the global community maturation cycle; Hallock *et al*. 1991; Hottinger 1998, 2001). Increasing oligotrophic conditions and a prominent sea level fall at 58.9 Ma (Hardenbol *et al*. 1998) favoured the proliferation of hermatypic coral build-ups throughout the Tethys (Tethyan platform stage I; Scheibner & Speijer 2008a, 2008b). Increasing global temperatures at the end of the Palaeocene caused a decline of many low-latitude coral communities (Tethyan platform stage II; Scheibner & Speijer 2008a, 2008b). The open niches were occupied by larger benthic foraminifera. Platform stage II represents a transitional episode between coralgal and larger foraminifera dominance in the Tethyan realm. In the northern Tethyan and peri-Tethyan realms, coralgal assemblages still dominated the platform margin, whereas at lower latitudes (0°–20°), larger foraminiferal communities composed of ranikothalids and miscellanids first proliferated. Duration was restricted to shallow benthic zone 4 (SBZ 4, Serra-Kiel *et al*. 1998).

1.2.2. Early Eocene

The Palaeocene–Eocene boundary represents a major caesura in the evolution of shallow marine benthic communities. The massive transient temperature peak during the Palaeocene–Eocene thermal maximum caused a Tethyan-wide decline of coral communities. Palaeocene ranikothalids and miscellanids were replaced by Eocene nummulitids and alveolinids (Scheibner *et al*. 2005). This evolutionary trend, known as larger foraminifera turnover, is directly linked to the negative carbon isotope excursion of the Palaeocene–Eocene thermal maximum (Orue-Etxebarria *et al*. 2001; Scheibner *et al*. 2005). Carbonate shelves were now dominated by photo-autotrophic larger benthic foraminifera assemblages throughout the Tethys (third phase of the global communifty maturation cycle; Hottinger 2001; Tethyan platform stage III; Scheibner & Speijer 2008a, 2008b). Studies from the Egyptian carbonate shelf suggest that the impact of the Early Eocene Climatic Optimum (52–49 Ma; Zachos *et al*. 2001) and the post-Palaeocene–Eocene Thermal Maximum hyperthermal events were of minor extent but may have coincided with a peak in the specific diversity of larger foraminifera K-strategists (organisms with a large body and a long live span that live in stable environments; Hottinger 1998; Hoentzsch *et al*. 2011b). Furthermore, the size of larger benthic foraminifera increased significantly from the Middle Ypresian to the Bartonian (fourth phase of the global community maturation cycle; Hottinger 2001).

1.2.3. Middle Eocene

The specific diversity of K-strategist larger benthic foraminifera continuously decreases from the base of the Lutetian to the Priabonian (Hallock *et al.* 1991; Hottinger 1998). The extinction of *Assilina* and giant *Nummulites* in the Lower Bartonian represents the termination of the Early Palaeogene global community maturation cycles (fifth phase; Hottinger 2001). The time interval from the Bartonian to the Priabonian is subdivided by Less and Özcan (2012) into 8 distinctive larger benthic foraminifera events related to climatic and evolutionary events.

A transient period with increasing abundance of larger benthic foraminifera K-strategist taxa is present during the Lower Bartonian (FO of Heterostegina; Less *et al*. 2008; Less & Özcan 2012) and represents the onset of a new global community maturation cycle (Hottinger 2001). This interval coincides with the transient warming during the Middle Eocene Climatic Optimum (MECO; Bohaty & Zachos 2003; Bijl *et al*. 2010).

The Lower Bartonian is characterised by prevailing oligotrophic conditions at the shelves (Nebelsick *et al*. 2005). The general cooling trend favoured the recovery of patchy coral communities in higher latitudes (Perrin 2002).

1.2.4. Late Eocene

A significant global temperature drop in the uppermost Middle Eocene (Middle/Late Eocene Cooling Event; McGowran 2009) accompanied by prevailing meso- to eutrophic conditions at the shelves caused a shift in the prevailing shallow benthic facies assemblages and a prominent demise of K-strategists (Hallock *et al.* 1991; Hottinger 2001). Oligotrophic symbiont-bearing larger benthic foraminifera (larger nummulitids, alveolinids, and acervulinids) were replaced by meso- to eutrophic coralline algae (Priabonian chronofauna; McGowran & Li 2001; Nebelsick *et al.* 2005). Despite the increasing availability of nutrients at the shelves, the recovery of coral communities continues, especially in the northern Tethyan realm (Nebelsick *et al.* 2005). The Thrace Basin in NW Turkey is a good example of this trend (Özcan *et al.,* 2010; Less *et al.,* 2011).

1.2.5. Early Oligocene

The tectonic and climatic isolation of Antarctica during the latest Eocene caused a massive temperature drop and the onset of perennial ice sheets in Antarctica (Oi-1 glaciation; Ivany *et al.* 2000; Zachos *et al.* 2001; Eldrett *et al.* 2009). Continuing cooling was accompanied by a strengthened ocean circulation and enhanced upwelling regimes (Hallock *et al.* 1991). This climatic and environmental caesura caused the extinction of larger benthic foraminifera that survived the Middle/Late Eocene Cooling Event (e.g., orthophragminids and early Palaeogene nummulites; Hallock *et al.* 1991; Prothero 2003). The newly created niche favoured the evolution of modern larger benthic foraminifera taxa and a slow diversification of Tethyan coral faunas (Hallock *et al.* 1991; Nebelsick *et al.* 2005). Newly emerged larger benthic foraminifera were represented by lepidocyclinids (FO upper Rupelian) and miogypsinids (FO Chattian; Özcan *et al.* 2010a).

1.3. Regional geological framework

1.3.1. Tectonic and stratigraphy at the South Iberian margin

The South Iberian continental margin has undergone repeated changes and deformation since the Mesozoic, culminating in the uplift and deformation of the Betic Cordillera orogen in the Early Miocene (Fontboté & Vera 1983; Blankenship 1992; Geel *et al.* 1998; Alonso-Chaves *et al.* 2004). Classical tectono-stratigraphic classifications differentiate an external zone, representing the autochthonous deposits of the South Iberian margin, and an internal zone, characterised by an allochthonous unit that underwent repeated metamorphism prior to the Early Miocene orogeny.

The external zone comprises a heterogeneous suite of Mesozoic and Early Cenozoic passive continental margin deposits (Garcia-Hernandez *et al.* 1980; Everts 1991). Those Triassic to Early Miocene sediments are detached from the Palaeozoic basement and have been thrust northward onto the southern margin of the Iberian Craton (Blankenship 1992). The deposits of the external zone are subdivided into 3 units with respect to their position at the shelf; the Prebetic domain represents the shallow marine shelf of the South Iberian margin, which is strongly affected by sea level variations and terrigenous input from the craton. Vast areas of the northern Prebetic were covered by a carbonate platform (Figure 2). The platform system represents a NE–SW striking belt of heterogeneous shallow marine sediments that were attached to the Iberian Massif. The southern Prebetic is rather influenced by hemipelagic deposition and frequent mass flows. The contact between the lagoonal Prebetic platform (External Prebetic) and the hemipelagic Prebetic realm (Internal Prebetic) is referred to as a major palaeogeographic barrier, called the Franja Anomala (e.g., de Ruig *et al.* 1991; Figure 3).

The Subbetic domain is characterised by deeper shelf deposits without major terrigenous influence (Figure 2). The contact between the Prebetic and Subbetic domains points to a major thrust fault (e.g. Garcia-Hernandez *et al.* 1980). The internal zone or Betic domain is characterised by a heterogeneous stack of allochthonous complexes containing thrust sheets of metamorphous Palaeozoic rocks (Geel 1996).

1.3.2. Tectonically controlled platform evolution during the Palaeogene

During the Early Palaeogene, the reactivation of major fault systems caused multiple phases of depositional instability and shelf reorganisation (Martin-Chivelet & Chacon 2007). A first tectonic phase is demonstrated for the Late Thanetian (Latest Thanetian Event, ~57 Ma; Martin-Chivelet & Chacon 2007), when a far field stress of strong compressional tectonics in the Pyrenean orogeny caused major block movement and a reorganisation of the South Iberian shelf basin. A major depositional unconformity at the Prebetic platform indicates there was a widespread subaerial exposure of the shallow marine shelf during that interval. An acceleration of the collisional tectonics of Africa and Iberia as well as the onset of the main orogenic phase in the Pyrenees resulted in a second tectonic phase during the Middle Ypresian (Intra-Ypresian event ~54.5 Ma; Martin-Chivelet & Chacon 2007). During the late Lutetian (Intra-Lutetian event, 44–42 Ma), a third tectonic phase resulted in a change of the major sediment transport direction along the platform from the N–S to the NE–SW and a significant progradation of the platform margin towards the south (Kenter *et al.* 1990). The continuing convergence between Africa and Eurasia caused a fourth phase during the Bartonian (Intra-Bartonian Event, 40–39 Ma), resulting in the tilting of the Prebetic platform. A fifth phase of major tectonic activity during the Late Eocene

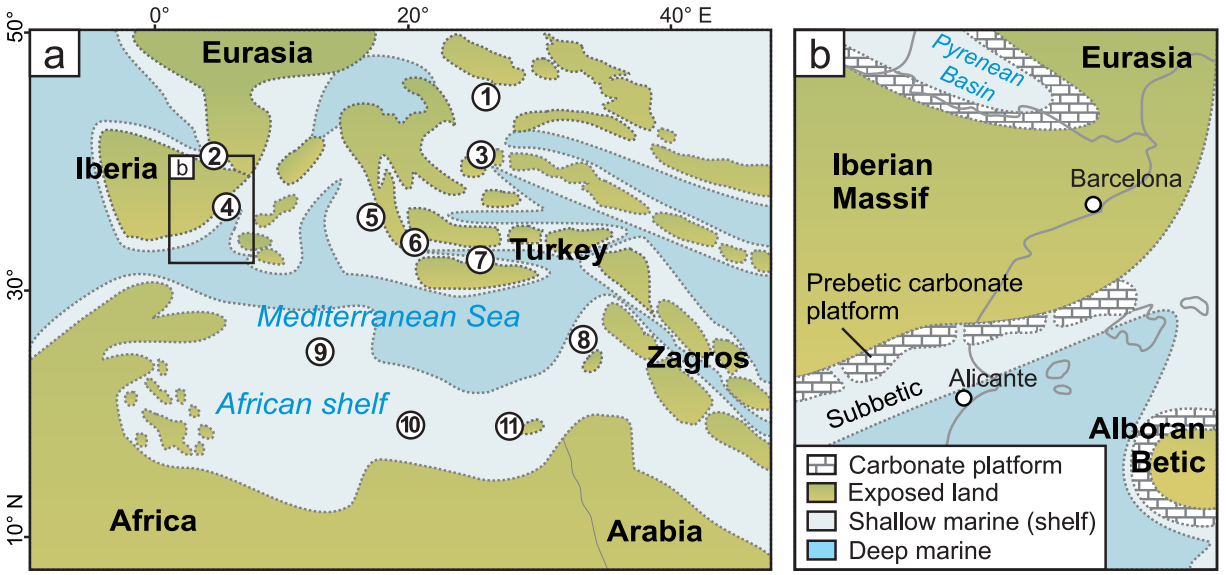

Figure 2a. Simplified palaeogeographic reconstruction of the Mediterranean realm in Early to Middle Eocene (Ypresian–Lutetian). Numbers indicate selected Eocene–Oligocene carbonate platform systems: 1) Northern Calcareous Alps, 2) Pyrenees, 3) North Adriatic platform, 4) Prebetic platform, 5) Maiella platform, 6) Greece, 7) Turkey, 8) NW Arabian platform (Syria, Israel), 9) Tunisia, 10) Libya (Sirte Basin), and 11) Egypt (Galala platform). The positions of the continents and ocean basins are adapted and expanded from Ziegler (1992), de Galdeano (2000), Meulenkamp and Sissingh (2000, 2003), and Thomas *et al.* (2010). **Figure 2b**. Early Palaeogene reconstruction of southern Iberian continental margin and the adjacent Alboran microplate, representing the (internal) Betic domain.

resulted in complex block-faulting of the platform and its separation into several isolated fault-bounded patch reefs with different subsidence levels and complex block topography (Intra-Priabonian event; De Ruig *et al.* 1991; Geel 1996; Geel *et al.* 1998). During the Oligocene, 2 more phases of tectonic activity have been suggested but not described in detail (Rupelian events).

The phases of major tectonic activity reveal a significant cyclicity in the depositional record of the South Iberian margin throughout the Palaeogene but especially during the Eocene. Geel *et al.* (1998) distinguish 14 third-order cycles in the Prebetic realm from the latest Palaeocene to the latest Eocene. Those cycles were mainly controlled by the tectonic processes related to the African–Eurasian collision and the far field impact of the Pyrenean orogeny. However, the beginning of glaciation in the southern hemisphere in the Late–Middle Eocene significantly increased the glacio-eustatic impact on the depositional record.

1.3.3. Regional climate of Iberia during the Palaeogene

The Palaeogene Iberian Peninsula was characterised by a stable microclimate due to the strong influence of the Tethys in the south and an emerging prominent orogenic system in the north (Postigo Mijarra *et al.* 2009). Early Cretaceous to Early Eocene conditions on the Iberian Peninsula were characterised by a tropical climate with seasonal rainfalls, evidenced by palaeotropical forests with a high floral diversity (Lopez-Martınez 1989; Gawenda *et al.* 1999; Adatte *et al.* 2000; Bolle & Adatte 2001; Postigo Mijarra *et al.* 2009). The impact of multiple Palaeogene hyperthermal events has been recorded in the Pyrenees (Angori *et al.* 2007; Scheibner *et al.* 2007; Alegret *et al.* 2009), the Basque Basin (Schmitz *et al.* 2001; Schmitz & Pujalte 2003), and the Betic realm (Alegret *et al.* 2010).

Large-scale tectonic reorganisation and the onset of the first ephemeral ice sheets in the southern hemisphere forced a global regression during the second half of the Eocene. This regression led to increasing aridity and continentalisation of the Iberian–Eurasian climate (Lopez-Martinez 1989).

2. Methods

Recording of 4 selected sections along a platform-to-slope transect was undertaken in order to establish a high-resolution dataset of various environments on the carbonate platform, comprising selected samples of mass flow deposits and hemipelagic background sediments. We recorded a new section of Ascoy in the SW part of the Prebetic platform and the classical sections of Oneil, Ibi, and Relleu for microfacies and biotic assemblages, comparable to the detailed microfacies analysis by Hoentzsch *et al.* (2011a). In this study, we only present the results of the microfacies and focus on a reinterpretation and comparison with other studies in order to achieve a

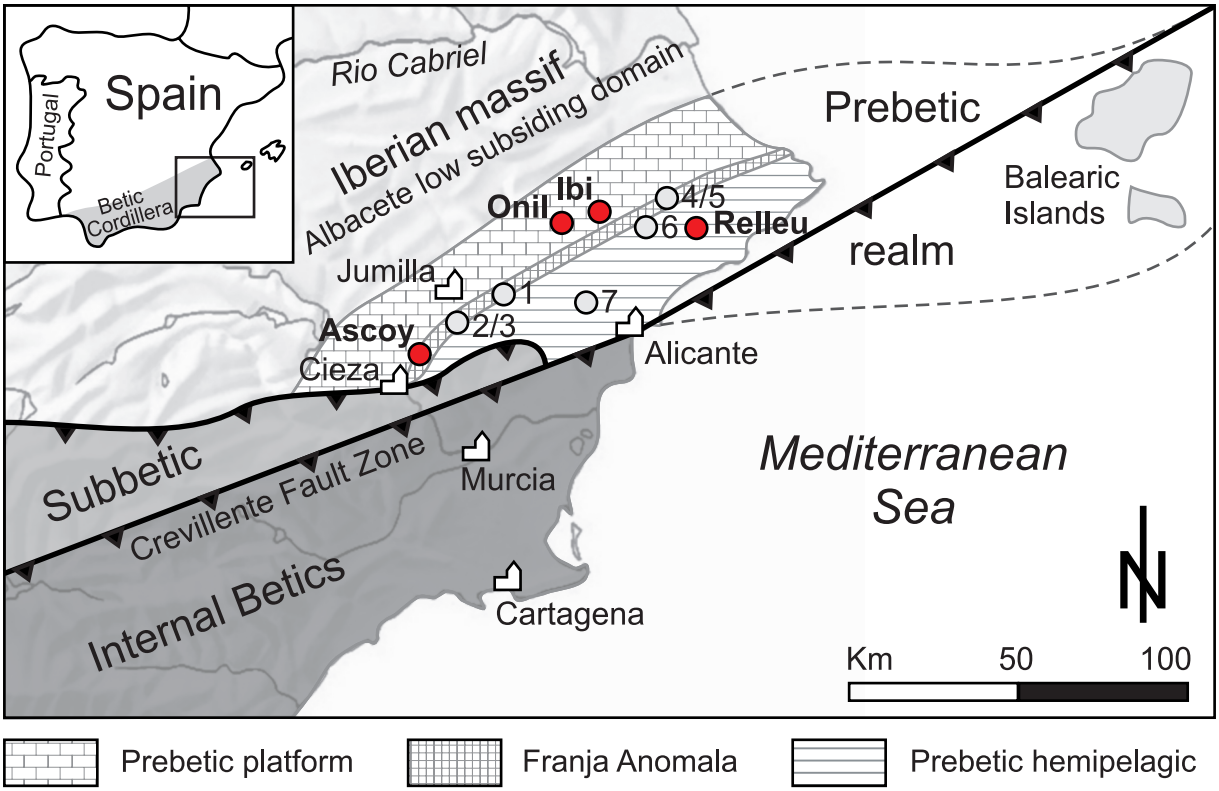

Figure 3. Location map of the eastern Betic Cordillera, including the main tectono-sedimentary units, major tectonic lineaments, and selected sections (modified after Martin-Chivelet and Chacon 2007). The contact between the Prebetic platform and the Prebetic hemipelagic realm is referred to as the Franja Anomala (e.g., de Ruig *et al.* 1991). Red circles indicate the location of the studied section; grey circles demonstrate previously studied Palaeogene sections of other authors (1 = Carche, 2/3 = Benis/Caramucel, 4/5 = Penaguila/Torremanzanas, 6 = Benifallim, and 7 = Agost).

coherent platform model with respect to depositional processes, climatic variability, and tectonic impact (Figure 3). Furthermore, limestones and marls from the lower slope section of the Relleu were analysed in order to record the long-term geochemical and carbon isotope evolution of a marginal shelf environment during times of major tectonic and climatic turnover. Bulk rock carbon isotopes ($\delta^{13}C$), total organic carbon (TOC), and calcite carbonate ratios were recorded and compared with data from the open ocean and similar marginal environments (Thomas *et al.* 1992; Zachos *et al.* 2001) in order to reveal either a coupling of the Prebetic platform to the global carbon cycle or the impact of regional processes on the Prebetic platform. To conclude, the main focus of this study is a continuation of the Tethyan carbonate platform evolution of Scheibner and Speijer (2008b) covering the Eocene to Early Oligocene.

For the isotope measurements, ground samples of bulk rock were prepared for measurement in a Finnigan MAT 251 mass spectrometer at the MARUM Centre for Marine Environmental Sciences (Bremen). It is a high-sensitivity, moderate-resolution magnetic sector mass spectrometer with an ion bombardment gas source.

Around 100 µg of sample material is needed for the procedure. The data obtained consist of isotopic proportions of oxygen and carbon in relation to the PDB standard. The measurement accuracy for the internal standard is given as under 0.05‰ for $\delta^{13}C$ and under 0.07‰ for $\delta^{18}O$. Therefore, any error made by measurement devices is assumed to be negligible.

The measurements of carbon content were done on ground bulk rock samples and measured 2 times in a Leco CS 200 carbon/sulphur analyser at the University of Bremen. Total carbon (TC) and total organic carbon (TOC) were each determined with one measurement. Around 50 mg of each sample was weighed into ceramic crucibles. TC was measured directly without further treatment of the sample whereas TOC samples were treated with diluted HCl (12.5%) beforehand. TOC samples were put under a fuel source for 2 to 3 days with the HCl to remove all inorganic bound carbon. The raw measured data are TC and TOC values. To get total inorganic carbon (TIC) values, the following equation was used: TIC = TC – TOC.

The total amount of $CaCO_3$ in the sample was computed based on this further equation:

$$CaCO_a[\%] = TIC \times \frac{a \times M(CaCOa_3)}{M(CO_3^{-2})}$$

Based on field experience and extensive microscopic observations, the possible influence of dolomitisation on the investigated rock samples is assumed to be negligible and is therefore not taken into account for the computation of TC.

3. Study area and data set

The Prebetic domain is a 130-km-long and 60-km-wide NE–SW striking fault-bounded block north and west of Alicante (Figure 3). It represents the northeasternmost part of the Betic Cordillera in SE Spain. North of the Prebetic domain, the Albacete low subsiding domain characterises the southern branch of the Iberian Massif. The Balearic Islands probably reflect a continuation of the Prebetics prior to the Late Oligocene to Neogene opening of the Balearic Sea (Doblas & Oyarzun 1990).

The Prebetic platform represents the northeasternmost part of the External Betics. Outcrops of the Palaeogene platform interior are rare due to frequent erosional and tectonic unconformities as well as intense karstification. Generally, sea level lowstands are missing in the depositional record on the platform (Geel 2000). In the southwesternmost part of the Prebetic domain, various isolated mountain ranges expose Palaeogene rocks, reflecting the transition from the inner shelf to the hemipelagic outer shelf (Carche, Benis, Enmedio; see Kenter *et al*. 1990). Outcrops along the deeper and more hemipelagic shelf are frequent in the areas of Relleu, Penaguila, Torremanzanas, and Benifallim (e.g., Everts 1991; Geel 2000) as well as the Agost section, representing the Internal Prebetics (e.g. Molina *et al*. 2000; Ortiz *et al*. 2008; Monechi & Tori 2010).

Most of the sections have been described and interpreted by various authors using different approaches. However, high-resolution microfacies and geochemical data are not available yet. In particular, the evolution of the platform interior and the impact of the environmental perturbations during and after the Paleocene–Eocene boundary have still not been described for the Prebetic platform.

3.1. Sections

We studied 4 sections of the Prebetic platform that are excellent examples for the coupled tectono-climatic impact on shallow marine benthic assemblages during the transition from Early Palaeogene greenhouse to Late Palaeogene icehouse conditions.

3.1.1. Section 1: Ascoy (Palaeocene–?Middle Eocene, ~120 m total thickness; Figure 4)

The Sierra d'Ascoy represents a WSW–ENE striking mountain range NE of Cieza. The depositional sequence encompasses Lower Cretaceous to Miocene hemipelagic marls and carbonates interrupted by several erosional unconformities (Kenter *et al*. 1990). Palaeogene rocks occur as a contiguous suite of Palaeocene to Middle Eocene carbonates of the platform interior, which merged into a transitional marine–continental facies during the Bartonian. Altogether, 78 limestone samples comprising larger benthic foraminifera, corals, and coralline red algae were collected. A few intervals show significant amounts of quartz grains. Palaeogeographic reconstructions of the Palaeogene integrate the succession of Ascoy to the Franja Anomala (Martinez del Omo 2003).

3.1.2. Section 2: Onil (Lowermost Eocene–Middle Eocene, ~210 m total thickness; Figure 4)

At the Onil section (~35 km N of Alicante), limestones and marls covering the lowermost Eocene to Middle Eocene are exposed and altogether 74 samples were collected. The rocks show a high abundance of larger benthic foraminifera (especially nummulitids and alveolinids) and reflect middle inner shelf settings during the Palaeogene. Geel (2000) describes 8 depositional cycles arranged in an overall shallowing-upward succession. The discrimination of the cycles is based on qualitative and quantitative variations in larger benthic foraminifera species as well as on detected erosional surfaces and hardgrounds. A few karstification horizons indicate temporarily subaerial exposure during sea level lowstands. The upper interval of the section is represented by dolomitised limestones.

3.1.3. Section 3: Ibi (Middle Eocene–Lower Oligocene, ~360 m total thickness; Figure 4)

The Ibi section represents a continuous succession of steeply tilted Middle Eocene to Middle Oligocene limestones and dolomites with rare marl intercalations. The section is situated about 35 km N of Alicante and about 10 km NE of the Onil section. Geel (2000) describes 8 Eocene cycles and 4 Oligocene cycles. Altogether, 130 samples were collected. The succession of Ibi is interpreted as platform interior or backreef environment and corresponds to the Onil section (Geel 2000).

3.1.4. Section 4: Relleu (Upper Eocene–Upper Oligocene, ~215 m total thickness; Figures 4 and 5)

The road-cut section of Relleu is situated ~35 km NE of Alicante and encompasses an alternating succession of hemipelagic marls and mass-flow related limestones. Limestones show a great variety of depositional textures (normal grading, flute casts, and rip-up clasts) that indicate a turbiditic origin. Furthermore, frequently transported larger benthic foraminifera from the inner platform (e.g., nummulitids and alveolinids) and autochthonous forms of orthophragminids are recorded. *Zoophycus* traces indicate a palaeo water depth of ~300 m that refers to the lower slope (Seilacher 1967; Everts 1991). The succession of Relleu encompasses 3 depositional sequences during the Eocene

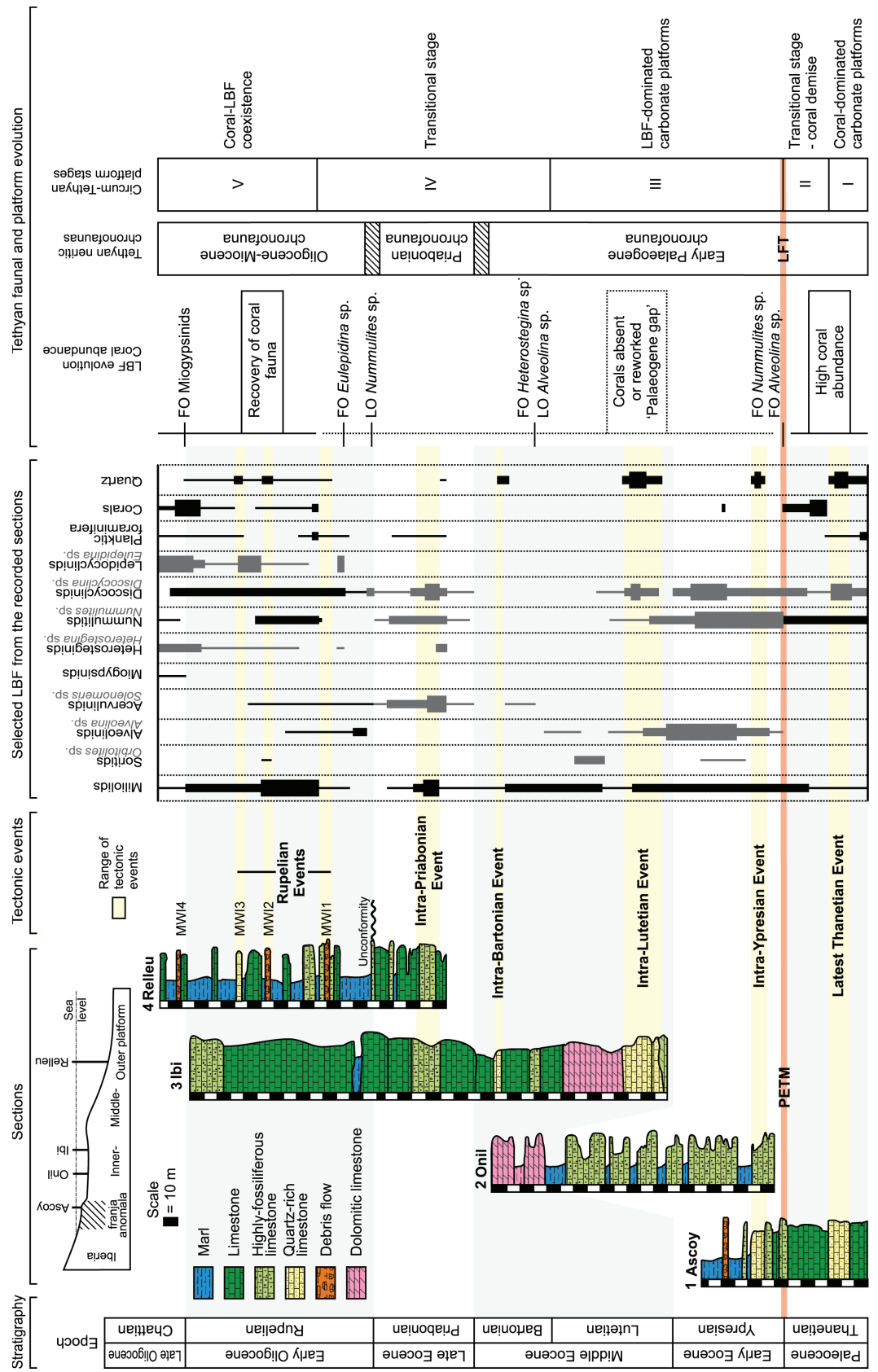

Figure 4. Faunal evolution of the Prebetic carbonate platform during the Palaeogene. The occurrence of selected larger benthic foraminifera specimens, corals, red algae, and quartz of 4 sections is summarised in order to demonstrate possible evolutionary turnover or extinctions. Palaeocene to Early Oligocene faunal evolution can be subdivided into 3 main intervals: a Palaeocene coral-dominated interval, an Early to Middle Eocene interval without coral records and larger benthic foraminifera-dominated assemblages, and a Late Eocene–Oligocene interval with increasing coral abundance but prevailing LBF assemblages. Abbreviations: FO = first occurrence, LO = last occurrence, MWI = mass wasting intervals (only for section Relleu), LFT = larger foraminifera turnover, and LBF = larger benthic foraminifera.

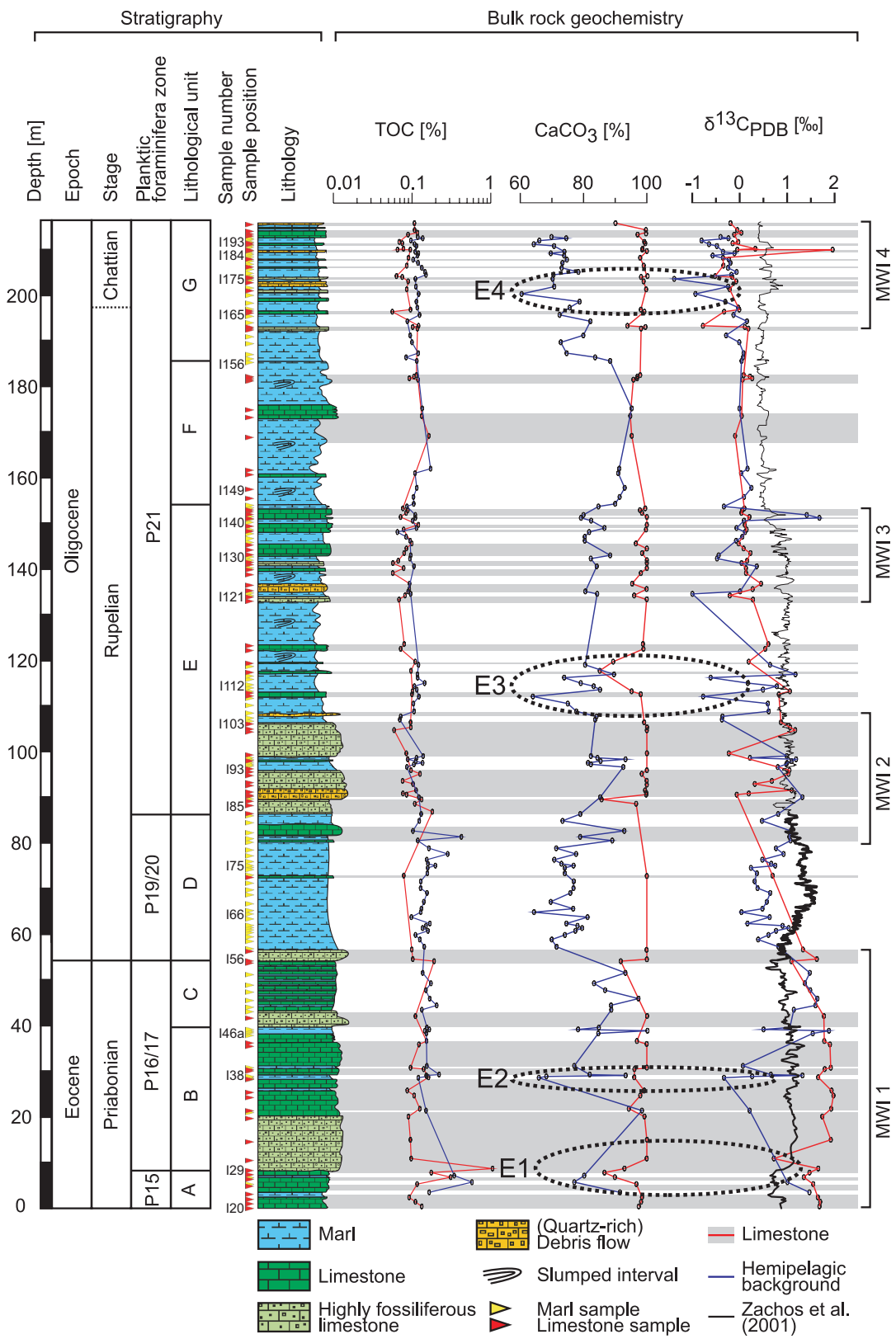

Figure 5. Bulk rock carbon isotopes and geochemistry for the Upper Eocene–Lower Oligocene outer ramp succession of Relleu. Data for hemipelagic background marls and limestones are plotted separately in order to show possible differences in source area and carbon burial. Grey bars indicate limestones. Mass wasting intervals (MWI) refer to periods of frequent turbidite deposition.

and 5 depositional sequences during the Oligocene (Geel 2000). In the Relleu section, 198 samples were collected.

The Eocene–Oligocene boundary and planktic foraminifera zone P18 are not recorded in the Relleu section. Geel (2000) relates this hiatus to a major erosional unconformity caused by the massive glacio-eustatic regression during the Oi-1 glaciation.

4. Results

4.1. The Palaeogene succession of the Prebetic platform

The 4 recorded sections represent a continuous succession of Palaeocene to Upper Oligocene platform deposits and hemipelagic marls. Depositional cycles at the Prebetic platform compiled by Geel *et al.* (1998) and Geel (2000) are renamed and used to describe the stratigraphic range of the recorded stratigraphic intervals (Figure 1). The recorded sections can be correlated by their biostratigraphic range or major tectono-depositional intervals (Figure 4).

4.1.1. Palaeocene (Thanetian)

Palaeocene rocks were only recorded at the Sierra d'Ascoy in the SW part of the Prebetic platform. The succession consists of massive fossiliferous limestones with high abundances of smaller rotaliid foraminifera, orthophragminids, coralline red algae (e.g., *Distichoplax biserialis*), echinodermal fragments, and highly disintegrated bioclasts. Smaller benthic foraminifera (miliolids) are rare. Detrital quartz accumulations of up to 20% are reported from a 15-m-thick massive siliciclastic limestone interval in the upper Thanetian (Figure 4; cycle T1). The quartz-bearing interval is followed by limestones with high abundances of hermatypic corals (cycle T2).

The Palaeocene–Eocene transition is represented by a significant shift in the shallow benthic faunal assemblage. Small rotaliids are replaced by larger nummulitids (*Operculina* sp., *Nummulites* sp.) and alveolinids (*Alveolina* sp.).

4.1.2. Early Eocene (Ypresian)

Lower Eocene rocks are recorded in the Ascoy and Onil sections. The basal Eocene succession of Ascoy is dominated by massive fossiliferous limestones with abundant large nummulitids, alveolinids, orthophragminids, and echinodermal fragments. Coralline algae are only common in the basal part of the Lower Eocene succession of the Ascoy (cycle Y1). Hermatypic corals are not recorded. In the Ascoy section, a significant quartz-bearing limestone bed in the middle Ypresian is strongly enriched with larger benthic foraminifera, shell fragments, and red algae (cycle Y1). During the upper Ypresian, fossiliferous limestones were replaced by marls with a thickness of up to 20 m (cycle Y2). Marls are intercalated by prominent massive limestone beds of 3–5-m thickness with reworked limestone nodules and high abundances of inner platform organisms (larger benthic foraminifera, coralline red algae, and echinoderm fragments).

The Lower Eocene succession of Onil is characterised by alternating highly fossiliferous limestones and marls. The recorded rocks are dominated by nummulitids (*Assilina* sp., *Nummulites* sp., and *Operculina* sp.), alveolinids (*Alveolina* sp.), orthophragminids, and echinoderm fragments. Soritids (*Orbitolites* sp.), miliolids, and serpulid worm tubes occur in varying amounts and accumulate in distinct intervals. Coralline red and green algae are rare. The dominance of orthophragminids decreased significantly during the Middle Ypresian.

4.1.3. Middle Eocene (Lutetian–Bartonian)

Middle Eocene rocks are recorded from the Onil and Ibi sections and can be divided into 3 major intervals. The basal Middle Eocene succession is characterised by partly dolomitised and quartz-rich limestones and marls without major fossil accumulations in the Onil section but by high fossil content in the Ibi section (cycles L1–L3).

The major benthic organisms in the Ibi limestones are orthophragminids, *Nummulites* sp., *Alveolina* sp., and *Assilina* sp.; miliolids; and soritids. The abundance of orthophragminids and nummulitids decreases significantly towards the upper part of the Middle Eocene succession (cycle L3). During cycle L4, an interval of massive-to-thick–bedded quartz-rich limestones up to 30 m in thickness and debris flow deposits with reworked limestones nodules and multiple erosional unconformities represents a major break in the deposition at the platform. Deposition after this mass wasting event is characterised by thickly bedded low fossiliferous nodular and dolomitised limestones (upper cycle L4/B). The first specimens of *Solenomeris* sp. are recorded in cycle B. The monotonous deposition is interrupted by a 2–4-m-thick interval of quartz-rich limestones (cycle B).

4.1.4. Late Eocene (Priabonian)

Upper Eocene rocks are recorded from the Ibi and Relleu sections. In contrast to the lightly fossiliferous upper interval of the Middle Eocene, the Upper Eocene successions of both sections demonstrate limestones and marls with high amounts of larger benthic foraminifera (*Nummulites* sp., orthophragminids, and *Solenomeris* sp.), smaller foraminifers (miolids), and bioclastic debris from the platform interior (gastropods, shell debris, echinoids, and coralline red algae). The first recorded specimen of *Heterostegina* sp. and the first Eocene coral fragments occur in cycle P1, which is younger than the occurrences of *Heterostegina* sp. in other Tethyan sections (Less *et al.* 2008; Less & Özcan 2012). A 10–15-m-thick interval of unconformably bounded highly fossiliferous and partly quartz-rich limestones is recorded for cycle P1.

4.1.5. Early Oligocene (Rupelian)

The Eocene–Oligocene boundary is only recorded at the Ibi section and refers to a major shift in the benthic assemblages. Post-Eocene shallow benthic organisms are

characterised by the first occurrence of lepidocyclinids (*Eulepidina* sp.) and nummulitids (*Heterostegina* sp.). Many Eocene larger benthic foraminifera (e.g., *Nummulites* sp., orthophragminids, and *Solenomeris* sp.) are not recorded from the Eocene–Oligocene boundary onwards, whereas miliolids and coralline red algae become more abundant. During cycle R2, the first hermatypic coral fragments are recorded since the lowermost Eocene. In the Relleu section, at least 3 intervals with increased deposition of debris flows and quartz-rich limestones are recorded (cycles R2–R4).

4.1.6. Late Oligocene (Chattian)

The Late Oligocene is only recorded in the uppermost intervals of the Relleu section and comprises marls and fossiliferous limestones. Limestones are rich in larger benthic foraminifera (*Eulepidina* sp. and *Heterostegina* sp.), red algal fragments, and coral debris.

4.2. Carbon isotope stratigraphy and geochemical evolution

The long-term bulk rock carbon isotope trend was only recorded for the Upper Eocene (Priabonian)–Upper Oligocene (Chattian) lower slope succession of Relleu (Figure 5; Table). This restriction to lower slope sediments minimises the possible effects of diagenesis, which might have a stronger influence on carbonate platform sediments due to the influence of meteoric waters during subaerial exposure. Carbonates and hemipelagic marls were examined separately in order to study the possible variations between the platform-derived turbidites and basinal hemipelagites.

4.2.1. Carbon isotopes

Marls: Bulk rock carbon isotopes from the recorded hemipelagic background deposits (marls) range from –1.5‰ to 1.5‰. The discrimination of significant trends is doubtful due to highly fluctuating carbon isotope ratios. The Priabonian is characterised by a prominent shift from positive to negative $d^{13}X$ ratios, culminating with a negative excursion of –0.5‰ and a fast recovery to 1‰ (E2; Figure 5). From the latest Priabonian to the Rupelian, the carbon isotope signature shifted from overall positive to negative ratios, superimposed by numerous minor positive and negative excursions. The depositional significance of those excursions is doubtful due to frequent slumping in the marl intervals. Chattian carbon isotopes ratios are characterised by a continuing shift towards negative $\delta^{13}C$ ratios with negative excursions in the lowermost interval of –1.5‰ (E4; Figure 5).

Limestones: The Priabonian is characterised by relatively stable positive $\delta^{13}C$ ratios (~1.5‰) with a negative excursion in lower mass wasting interval 1 (MWI 1; E1; Figure 5). Carbon isotopes from the recorded Priabonian limestones indicate strong variations compared to the $\delta^{13}C$ of the measured hemipelagic marls. During the uppermost Priabonian, carbon isotope ratios shifted to more negative ratios in the limestones. This trend continued during the Rupelian with minor excursions during MWI 2. During the upper Rupelian and Chattian, $\delta^{13}C$ ratios of both marl and limestone units converged and showed only minor variations.

4.2.2. Calcium carbonate ratios

Marls: Bulk rock calcium carbonate ratios vary significantly between the recorded limestones and marls. In the upper Priabonian (P16/17), marls show $CaCO_3$ ratios between 80% and 96% with transient drops to ~65% at 28 m above the base of the section). This significant excursion correlates with a negative carbon isotope peak.

The Eocene–Oligocene transition is marked by a 10%–15% drop in the calcium carbonate ratios of the hemipelagic background marls. Average $CaCO_3$ ratios range from 70% to 80% in the lowermost Rupelian (P19/20) and increase to ~90 % in P21. In lower P21, a transient $CaCO_3$ drop from ~90% to 63% correlates with 2 minor negative carbon isotope peaks (E3; Figure 5). The calcium carbonate trend in the upper Rupelian and lowermost Chattian (upper P21) is characterised by a continuous decrease from >90% to <70%.

Limestones: The recorded limestones show only minor fluctuations in the $CaCO_3$ content with ratios between 95% and 100%. Three intervals with transient calcium carbonate drops to 85% are recorded at the basis of P16 (E1; Priabonian), at the basis of P21 (Rupelian), and in the lower part of P21 (E3).

4.2.3. Total organic carbon (TOC)

Bulk rock TOC ratios do not show any significant trends in the marls or in the limestones throughout the recorded succession. Average TOC ratios range from 0.05% to 0.15%. A prominent excursion of 0.75% in the TOC ratios is recorded at the base of P16 (Priabonian). This prominent TOC excursion correlates with a ~4-m-thick interval of transient decreased $CaCO_3$ ratios and a significant negative carbon isotope excursion in the recorded limestones (E1; Figure 5).

5. Discussion

5.1 Circum-Tethyan carbonate platform evolution during the Palaeogene—the Prebetic platform as a test case

The biotic evolution of the Prebetic carbonate platform can be characterised by major shifts in the prevailing benthic assemblages (Figure 4). Those shifts are related to climatic and environmental trends (temperature and nutrient availability), which cause the emergence, proliferation, and demise of environmentally sensitive platform organisms. Excellent palaeoenvironmental indicators at the Prebetic platform are represented by corals, larger benthic foraminifera, and coralline red

Table. Geochemical data for section Relleu.

Sample #	Depth [m]	Thin section	Sample association	$6^{13}C$ [‰]	Carbon [%]	TOC [%]	$CaCO_3$ 100%
I 20	0.5	yes	mass flow	1.69	11.795	0.09	97.47
I 21	1.5	yes	mass flow	1.70	11.866	0.08	98.19
I 22	2.5	yes	mass flow	1.65	11.887	0.07	98.48
I 23	3.6	yes	background	1.48	11.102	0.12	91.51
I 24	5.4	yes	mass flow	1.55	11.691	0.08	96.70
I 25	5.8	no	background	1.01	9.6628	0.41	77.09
I 26	6.9	yes	mass flow	1.36	11.012	0.22	89.91
I 27	7.25	no	background		9.8731	0.24	80.22
I 28	7.9	yes	mass flow	1.48	10.521	0.12	86.60
I 29	8.8	yes	mass flow	1.66	11.902	0.75	92.93
I 12	11	yes	mass flow	0.73	12.209	0.07	101.13
I 30	15.1	yes	mass flow	1.93	12.266	0.07	101.61
I 31	20.2	yes	mass flow	1.75	11.979	0.06	99.25
I 32	21.5	no	background	0.22	11.927	0.11	98.46
I 33	21.9	yes	mass flow	1.93	11.412	0.09	94.32
I 34	24.8	yes	mass flow	1.98	11.832	0.08	97.93
I 35	25.9	yes	mass flow	1.94	11.965	0.06	99.16
I 36	28.7	no	background	–0.32	7.992	0.09	65.86
I 37	28.8	yes	mass flow	1.66	11.644	0.11	96.04
I 38	29	no	background	0.27	8.3014	0.11	68.24
I 39	29.2	no	background	1.33	11.308	0.11	93.30
I 40	29.4	no	background	0.66	9.9946	0.16	81.95
I 40a	30.6	yes	mass flow	1.80	11.635	0.10	96.09
I 41	30.9	yes	mass flow	1.93	12.209	0.07	101.14
I 42	31.3	no	background	0.08	9.3608	0.11	77.07
I 43	36	yes	mass flow	1.91	12.197	0.09	100.88
I 44	36.75	yes	mass flow	1.79	11.739	0.11	96.89
I 45	38.4	no	background	1.55	10.272	0.11	84.67
I 46	39	no	background	1.89	12.131	0.10	100.19
I 46a	39.3	no	background	0.51	9.5125	0.12	78.26
I 47	39.7	no	background	1.06	10.295	0.11	84.85
I 48	42.2	yes	mass flow	1.78	12.161	0.08	100.65
I 49	43.6	no	background	1.15	10.751	0.09	88.77
I 50	44.55	no	background	1.60	10.792	0.15	88.68
I 51	46.05	no	background	1.64	11.807	0.12	97.36
I 52	47.9	no	background	1.49	10.527	0.11	86.81
I 53	49.4	no	background	1.38	10.126	0.12	83.32
I 54	51.7	no	background	1.48	11.289	0.10	93.23
I 55	54.25	yes	mass flow	1.10	11.151	0.13	91.76
I 56	54.7	yes	mass flow	1.63	12.221	0.07	101.20
I 57	56.8	yes	mass flow	1.34	12.246	0.07	101.42
I 58	57.4	no	background	0.82	8.6821	0.10	71.48
I 59	59	no	background	0.40	8.4844	0.09	69.94
I 60	60	no	background	0.61	8.9748	0.08	74.11
I 61	60.9	no	background	0.77	9.406	0.11	77.41
I 62	61.5	no	background	1.04	9.6452	0.10	79.54

Table. (continued).

Sample #	Depth [m]	Thin section	Sample association	$\delta^{13}C$ [‰]	Carbon [%]	TOC [%]	$CaCO_3$ 100%
I 63	62	no	background	0.91	9.4809	0.11	78.09
I 64	62.5	no	background	0.17	9.0714	0.12	74.57
I 65	63.9	no	background	0.64	9.8243	0.07	81.26
I 66	65	no	background	0.04	7.8141	0.09	64.33
I 67	65.75	no	background	0.49	9.3033	0.09	76.72
I 68	67.25	no	background	0.58	8.4588	0.10	69.63
I 69	69.2	no	background	0.65	9.2117	0.11	75.82
I 70	70.25	no	background	0.38	9.3132	0.09	76.82
I 71	71.75	no	background	0.32	9.3231	0.09	76.90
I 72	73	yes	mass flow	0.70	12.106	0.06	100.38
I 73	73.5	no	background	0.37	9.0045	0.11	74.09
I 74	74.7	no	background	0.24	9.0034	0.11	74.07
I 10	75.2	no	background	0.75	9.3654	0.14	76.85
I 75	75.6	no	background	0.67	8.8766	0.11	73.00
I 76	76.5	no	background	0.48	8.602	0.11	70.75
I 77	77.75	no	background	0.93	9.5223	0.20	77.65
I 78	79	no	background	0.77	8.6834	0.12	71.37
I 79	80.7	no	background	1.08	10.778	0.08	89.08
I 80	81.5	no	background	1.05	9.7749	0.30	78.93
I 81	82.8	no	background	1.08	11.223	0.07	92.88
I 82	85	no	background	0.48	8.8936	0.09	73.36
I 83	86.5	no	background	0.82	9.5717	0.09	78.96
I 84	87	yes	mass flow		6.0862	0.13	
I 85	88.75	yes	mass flow		11.677	0.08	96.63
I 86	89.7	yes	mass flow		10.383	0.09	85.71
I 87	90.2	no	background	1.33	10.322	0.09	85.26
I 88	90.75	yes	mass flow	–0.05	12.042	0.06	99.81
I 88a	91	yes	mass flow	0.20	12.218	0.05	101.32
I 89	91.7	yes	mass flow	1.10	12.02	0.08	99.46
I 9	93.1	yes	mass flow	0.33	12.262	0.07	101.54
I 90	93.75	yes	mass flow	0.68	12.162	0.05	100.86
I 91	95.3	yes	mass flow	1.04	11.904	0.09	98.42
I 92	96.1	yes	mass flow	1.05	12.076	0.07	100.02
I 93	96.8	yes	background	0.81	11.172	0.06	92.56
I 94	97.4	no	background	0.99	9.958	0.07	82.33
I 95	97.7	no	background	1.00	9.8689	0.10	81.40
I 96	98.1	no	background	1.10	10.33	0.08	85.39
I 97	98.5	yes	background	1.19	11.258	0.06	93.26
I 98	98.8	no	background	0.22	10.212	0.08	84.39
I 99	99.2	no	background	1.00	9.9803	0.10	82.32
I 100	99.8	yes	mass flow	–0.22	12.18	0.06	100.96
I 101	104.9	yes	mass flow	1.18	12.152	0.04	100.88
I 102	105.5	yes	mass flow	1.07	12.082	0.07	100.07
I 103	106.6	yes	mass flow	0.88	11.973	0.07	99.17
I 104	107.2	no	background	–0.37	10.094	0.05	83.67
I 105	107.9	no	background	–0.36	10.147	0.05	84.10
I 106	109	no	background	0.62	9.4023	0.08	77.70
I 107	110.7	no	background	0.60	9.079	0.07	75.01
I 108	112.25	no	background	–0.76	7.7674	0.09	63.98

Table. (continued).

Sample #	Depth [m]	Thin section	Sample association	$\delta^{13}C$ [‰]	Carbon [%]	TOC [%]	$CaCO_3$ 100%
I 8	112.75	yes	mass flow	0.83	11.844	0.07	98.07
I 109	113.4	yes	mass flow	1.06	11.499	0.07	95.19
I 110	113.75	no	background	0.50	10.31	0.08	85.20
I 111	114.5	no	background	0.79	10.065	0.08	83.21
I 112	115.2	no	background	0.18	9.6004	0.10	79.12
I 113	116.4	no	background	–0.61	8.9521	0.08	73.88
I 114	117.1	no	background	1.18	10.842	0.08	89.62
I 115	117.9	yes	mass flow		10.288	0.07	85.13
I 116	119.2	no	background	0.65	9.7487	0.09	80.50
I 117	119.9	yes	mass flow	0.20	10.807	0.08	89.38
I 118a	122.7	yes	mass flow	0.54	11.928	0.05	98.94
I 118	123.75	yes	mass flow	0.61	11.915	0.06	98.78
I 119	133.5	yes	mass flow	0.29	12.103	0.05	100.42
I 120	134.4	yes	mass flow	–0.20	11.582	0.06	96.00
I 121	134.75	no	background	–0.99	10.189	0.07	84.31
I 122	135.3	no	background	0.01	9.7346	0.06	80.56
I 7	135.8	yes	mass flow	0.28	12.413	0.07	102.86
I 123	137	yes	mass flow	0.45	11.516	0.07	95.38
I 124	139.3	yes	mass flow	0.14	11.821	0.04	98.13
I 6	140.4	yes	mass flow	0.14	12.102	0.06	100.35
I 126	140.8	no	background	0.37	10.179	0.07	84.17
I 127	141.5	yes	mass flow	0.05	12.047	0.04	100.01
I 128	142	yes	mass flow	0.16	12.247	0.05	101.62
I 129	142.5	no	background	–0.47	9.9462	0.07	82.30
I 130	143.2	no	background	–0.44	10.681	0.07	88.41
I 131	143.7	yes	mass flow	0.23	11.883	0.06	98.52
I 132	144.7	yes	mass flow	0.09	12.139	0.06	100.62
I 133	145.8	yes	mass flow	–0.02	11.661	0.07	96.55
I 134	146.4	no	background	–0.07	9.7182	0.07	80.40
I 135	147.25	no	background	0.06	9.7102	0.06	80.39
I 136	148.3	no	background	0.12	9.8615	0.05	81.76
I 137	148.85	yes	mass flow	0.15	12.028	0.06	99.73
I 138	149.2	no	background	–0.06	10.478	0.08	86.61
I 139	149.9	yes	mass flow	0.11	12.119	0.09	100.24
I 140	150.8	no	background	0.10	9.9639	0.07	82.40
I 141	151.4	no	background	1.69	9.5837	0.08	79.18
I 142	151.6	yes	mass flow	0.21	12.09	0.05	100.29
I 143	152.05	no	background	1.42	9.6793	0.08	79.98
I 144	152.5	yes	mass flow	0.04	11.881	0.06	98.47
I 5	153.1	yes	mass flow	0.06	11.809	0.06	97.85
I 145	153.5	yes	mass flow	0.10	11.999	0.05	99.50
I 146	153.9	no	background	–0.33	10.23	0.06	84.71
I 147	154.5	no	background		10.878	0.07	89.99
I 148	156	yes	background	0.10	11.047	0.07	91.41
I 149	158	yes	background	0.25	11.247	0.08	93.01
I 150	161.2	yes	background	0.03	10.999	0.08	90.98
I 151	162.2	yes	background	0.17	11.08	0.12	91.28
I 152	169.4	yes	mass flow	–0.09	11.549	0.12	95.24
I 153	173.75	yes	mass flow	0.05	11.471	0.09	94.77
I 154	175.4	yes	background	0.00	11.527	0.10	95.23

Table. (continued).

Sample #	Depth [m]	Thin section	Sample association	$\delta^{13}C$ [‰]	Carbon [%]	TOC [%]	$CaCO_3$ 100%
I 155b	181.7	yes	mass flow	0.07	11.581	0.08	95.77
I 155a	182	yes	mass flow	0.27	11.699	0.07	96.91
I 155	182.4	yes	mass flow	0.22	11.726	0.08	97.05
I 4	182.7	yes	mass flow	0.09	11.834	0.08	97.91
I 156	185.8	no	background	0.05	10.694	0.08	88.40
I 157	186.6	no	background	0.08	10.102	0.06	83.65
I 158	187.5	no	background	0.09	9.046	0.08	74.65
I 159	189.9	no	background	0.00	8.8091	0.07	72.79
I 160	191.4	no	background	–0.28	9.663	0.07	79.93
I 161	192.9	yes	mass flow	0.19	11.871	0.08	98.20
I 3	193.25	yes	mass flow	0.11	12.024	0.07	99.56
I 162	193.5	yes	mass flow	–0.77	11.354	0.09	93.87
I 163	194.5	no	background	0.16	9.9245	0.06	82.16
I 164	195.9	no	background	–0.12	8.7809	0.09	72.41
I 165	196.6	yes	mass flow	–0.32	11.951	0.04	99.22
I 166	197.05	yes	mass flow	0.00	11.847	0.07	98.12
I 167	197.5	no	background	–0.03	9.1573	0.08	75.59
I 168	198.8	no	background	–0.30	9.5339	0.08	78.75
I 169	200.5	no	background	–0.93	7.3402	0.09	60.43
I 170	201.5	yes	mass flow	–0.21	12.04	0.06	99.79
I 171	202.1	no	background	–0.24	8.5708	0.08	70.73
I 172	203.25	yes	mass flow	–0.07	11.947	0.06	98.99
I 173	203.8	no	background	–1.37	8.5103	0.08	70.24
I 174	204.2	yes	mass flow	–0.15	11.84	0.05	98.18
I 175	204.4	yes	mass flow	–0.51	12.076	0.04	100.22
I 176	204.7	no	background	–0.17	8.569	0.11	70.49
I 177	205.3	no	background	–0.06	9.5124	0.10	78.38
I 178	206.2	no	background	–0.24	8.8694	0.09	73.10
I 178b	206.7	yes	mass flow	–0.34	11.948	0.06	99.02
I 179	207.3	no	background	–0.19	8.8882	0.08	73.34
I 180	208	no	background	–0.22	9.043	0.07	74.72
I 181	208.4	yes	mass flow	–0.35	11.818	0.06	97.91
I 182	208.9	no	background	–0.56	8.9529	0.08	73.89
I 183	209.4	no	background	–0.10	8.4462	0.09	69.65
I 184	209.75	no	background	–0.35	8.9557	0.08	73.95
I 2	210.2	yes	mass flow	1.96	12.374	0.07	102.52
I 185	210.2	yes	mass flow	–0.04	11.88	0.05	98.58
I 186	210.4	yes	mass flow	0.34	11.898	0.06	98.65
I 187	211	no	background	–0.47	8.5661	0.08	70.69
I 188	211.4	no	background	–0.64	7.7918	0.08	64.27
I 189	211.6	yes	mass flow	–0.14	11.998	0.05	99.50
I 190	211.9	yes	mass flow	–0.02	11.958	0.05	99.20
I 191	212.2	no	background	–0.80	7.9937	0.07	66.02
I 192	212.7	no	background	–0.23	9.0422	0.10	74.52
I 193	213	no	background	–0.40	8.4709	0.08	69.87
I 194	213.5	yes	mass flow	–0.11	11.719	0.06	97.09
I 195	213.9	yes	mass flow	0.04	13.438	0.08	111.25
I 196	214.5	yes	mass flow	–0.04	12.048	0.08	99.72
I 1	216	yes	mass flow	–0.19	10.892	0.08	90.10

algae. Coral reefs represent highly sensitive ecosystems with clearly defined thresholds regarding thermal stress, eutrophication, and turbidity (Hallock 2005; Payros *et al.* 2010). Increasing global temperatures during the Early Palaeogene (58–49 Ma) with low latitudinal gradients and generally low Mg/Ca ratios in the ocean water hampered the growth of larger coral communities, while larger benthic foraminifera proliferated (Scheibner & Speijer 2008a, 2008b). Furthermore, the aragonitic skeleton of corals is more prone to calcium carbonate dissolution than the calcitic tests of larger benthic foraminifera (Payros *et al.* 2010). The transition from coral-dominated assemblages to larger benthic foraminifera-dominated assemblages can be observed at the Prebetic platform and throughout the Tethys (Figure 4), although timing and distribution are strongly linked to latitude (Figure 6). The 3 major circum-Tethyan platform stages arranged by Scheibner and Speijer (2008a) pinpoint the climatically controlled trends in larger benthic foraminifera and coral evolution from the Late Palaeocene to the Early Eocene. Platform stage I (58.9–56.2 Ma; SBZ 1–3) is represented by the dominance of coralgal assemblages throughout the Tethys. Platform stage II (56.2–55.5 Ma; SBZ 4) represents a transitional stage with prevailing corals in the northern Tethyan realm but a significant demise of coral build-ups in the southern Tethys. During platform stage III (55.5–?; SBZ 5/6–?), larger benthic foraminifera replaced corals as major platform organisms.

The demise of coral-dominated platforms during the Palaeocene is rather an effect of coupled long-term climatic evolution and multiple transient environmental perturbations. With the pronounced sea surface temperature rise at the Palaeocene–Eocene Thermal Maximum and the coeval eutrophication of shelf areas, the living conditions of corals probably exceeded a critical threshold throughout the Tethys, whereas the long-term coral demise during the Late Palaeogene is only an effect of increasing greenhouse conditions.

However, Scheibner and Speijer (2008a) only define platform stage III as a tentative interval with a stratigraphic range of less than 500 ky. The timing of the recovery of the circum-Tethyan coral fauna and, thus, the range of platform stage III are still under debate. Hoentzsch *et al.* (2011b) show that benthic foraminifera dominated in the low latitude carbonate shelf of Egypt at least until the end of the Early Eocene Climatic Optimum (~49 Ma, SBZ 14a). New data from the Prebetic platform in SE Spain and compiled records from numerous Eocene–Oligocene shallow marine successions reveal the evolution of circum-Tethyan carbonate platforms during the transition from a global greenhouse to an icehouse (Figures 6 and 7).

We selected 11 Palaeocene to Oligocene carbonate platform systems in the Tethys that provide sufficient data for a comparison between the abundance of corals and larger benthic foraminifera. The selected environments range from temperate latitudes (~25°N to 43°N) to equatorial latitudes (<25°N). Especially in the northern cool temperate environments (e.g., Northern Calcareous Alps, Prebetic platform), carbonates are frequently dominated by coralline algae, which are associated with larger benthic foraminifera (Rasser 1994; Rasser & Piller 2004; Nebelsick *et al.* 2005). However, major platform organisms besides larger benthic foraminifera and corals are not considered in this approach, due to their high thresholds to temperature and nutrient fluctuations.

1) Northern Calcareous Alps (43°N)

Shallow-benthic assemblages in the Northern Calcareous Alps show a significant demise of hermatypic corals and a coeval increase in larger benthic foraminifera after the Palaeocene–Eocene thermal maximum (Darga 1992; Schuster 1996b; Scheibner & Speijer 2008b). However, the coral fauna did not disappear in the Early Eocene and persisted in rare small patch reefs until the Bartonian, whereas larger benthic foraminifera remained a major platform contributor. During the Priabonian, the coral abundance increased significantly. Corals proliferated throughout the Northern Calcareous Alps and formed major reefs (Nebelsick *et al.* 2005).

2) Pyrenees (38°N)

The Pyrenean succession has been strongly affected by the compressional tectonics of Iberia and Eurasia since the Mesozoic (Vergés *et al.* 2002). Continuous Palaeogene sections are rare and often influenced by terrigenous deposits. However, various studies show flourishing coral patch reefs during the Early Eocene (Eichenseer & Luterbacher 1992; Schuster 1996a). Bartonian successions are rare and indicate larger benthic foraminifera as major platform building organisms (Payros *et al.* 2010). Abundant corals are described within siliciclastic mesotrophic prodelta settings in the Priabonian (Morsilli *et al.* 2012). The ongoing Pyrenean orogeny led to an increasing continental infill of the Pyrenean basins and the destruction of the platform during the upper Priabonian and Oligocene (Vergés *et al.* 2002).

3) North Adriatic platform (38°N)

The Palaeogene succession of the North Adriatic platform reveals the existence of larger benthic foraminifera-dominated assemblages without corals during the Ypresian and Lutetian (Cosovic *et al.* 2004; Zamagni *et al.* 2008). The first coral records after the Palaeocene–Eocene Thermal Maximum point to the uppermost Lutetian (SBZ 16; Cosovic *et al.* 2004). A significant increase in coral abundance is recorded from the Early Oligocene in successions in Slovenia and in the Po Basin (Nebelsick *et al.* 2005).

4) Prebetic platform (36°N)

The Prebetic platform is dominated by larger benthic foraminifera assemblages without coral records

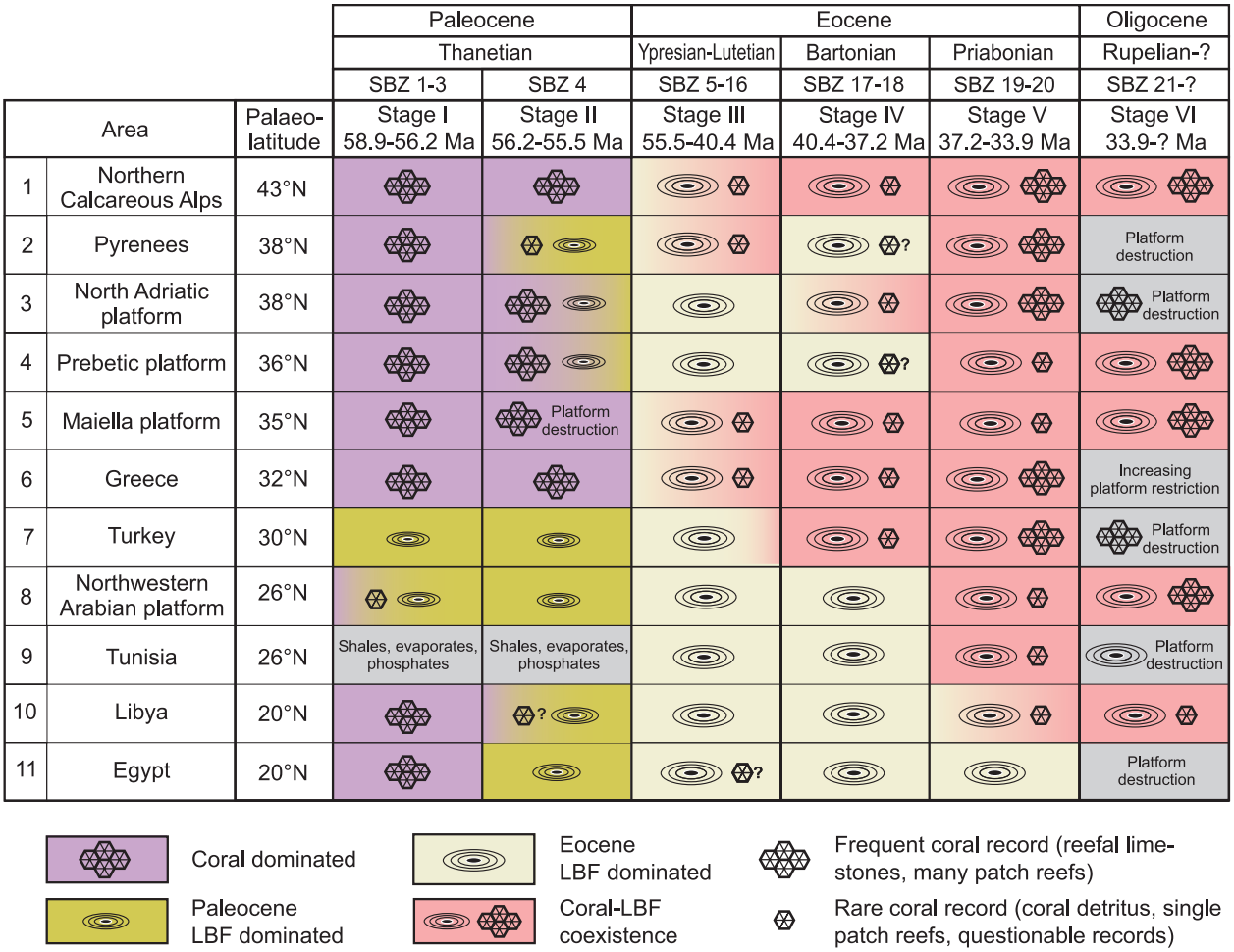

Figure 6. The evolution of circum-Tethyan carbonate platforms with respect to the latitudinal and quantitative distribution of larger benthic foraminifera (LBF) and major coral built-ups. Question marks refer to very rare or questionable coral records. Platform stages I–III according to Scheibner and Speijer (2008a). Shallow-benthic zonations (SBZ) refer to the classifications of Cahuzac and Poignant (1997) for the Oligocene and Serra-Kiel *et al.* (1998), Less *et al.* (2008), and Less and Özcan (2012) for the Palaeocene and Eocene.

throughout the Early and Middle Eocene (Geel 2000; this study). Increasing abundance of coral fragments and the first post-Palaeocene–Eocene Thermal Maximum patch reefs were present during the Late Eocene (Geel 2000; this study).

5) Maiella platform (35°N)

Platform deposits of the Maiella platform are dominated by larger benthic foraminifera in the Early and Middle Eocene (Moussavian & Vecsei 1995; Vecsei & Moussavian 1997). Corals are generally present but are not considered to be a major platform contributor. Extend coral reefs are described from the Priabonian and Oligocene (Vecsei & Sanders 1997). The timing of major coral abundance during the Priabonian coincides with coral-solenomeris assemblages in the Trentino in North Italy (SBZ 20; Bassi 1998; Bosellini & Papazzoni 2003)

6) Greece (32°N)

Accordi *et al.* (1998) describe environments dominated by larger benthic foraminifera shoals with colonial coral fragments during the Early Eocene. The first recorded reefal limestones with major coral abundance point to the Late Bartonian and Priabonian (Barattolo *et al.* 2007). The Oligocene is characterised by an increasing restriction of the shallow marine environment and the concurrent destruction of the platform (Barattolo *et al.* 2007).

7) Northern and Central Turkey (30°N)

Studies on carbonate platforms from the Palaeogene of northern and central Turkey reveal a strong tectonic influence and highly discontinuous sections. The Thrace Basin in NW Turkey was dominated by larger benthic foraminifera during the Early Eocene. The first coral reefs records are dated from the late Lutetian to early Bartonian

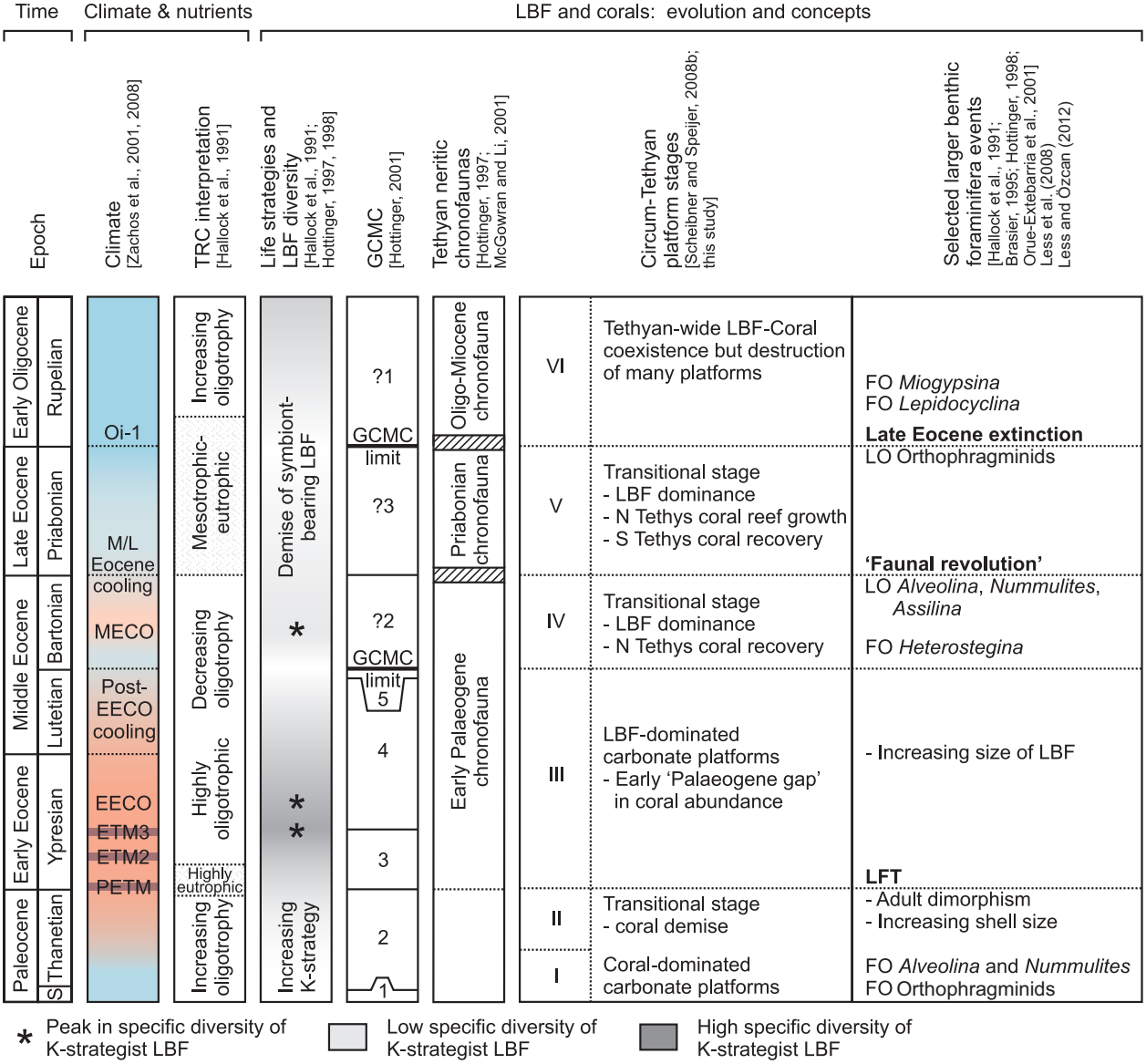

Figure 7. Relationship between circum-Tethyan platform stages and climate, climatic events, trophic resources, larger benthic foraminifera, and coral evolution during the Palaeogene. Main evolutionary caesuras are represented by major climatic events (Palaeocene–Eocene thermal maximum, Middle–Late Eocene cooling event, Oi-1 glaciation). The global community maturation cycle limit at the Lutetian–Bartonian boundary is probably linked to the increasing availability of nutrients at the shelves. Abbreviations: S = Selandian, ETM = Eocene thermal maximum, FO = first occurrence, LO = last occurrence, GCMC = global community maturation cycle, LBF = larger benthic foraminifera.

(Middle Eocene; Özcan *et al.* 2010; Less *et al.* 2011), although the most prominent patch reefs occur in the late Bartonian to Priabonian (Middle–Late Eocene; Özcan *et al.* 2010; Less *et al.* 2011). Other authors conclude the late Early Oligocene was a period with the first coral records in the area (SBZ 21/22; Schuster 2002; Harzhauser 2004; İslamoğlu *et al.* 2010).

8) Northwestern Arabian platform (26°N)

The NW Arabian Platform (or Levant Platform) is dominated by nummulitic limestones from the Early Eocene to the Priabonian (Ziegler 2001; Daod 2009). Small Early Eocene patch reefs are recorded in Israel (Benjamini 1981). Krasheninnikov (2005) describes Upper Eocene and Oligocene coral-bearing reefal limestones in the Palmyrids of Syria. In Israel, the first coral records after the Palaeocene–Eocene thermal maximum correspond to the Late Eocene (Benjamini & Zilberman 1979).

9) Tunisia (26°N)

Early to Middle Eocene rocks are dominated by nummulitic limestones without hermatypic corals

(Bismouth & Bonnefous 1981; Loucks *et al.* 1998; Beavington-Penney *et al.* 2005; Taktak *et al.* 2010; Tlig *et al.* 2010). The first rare coral records are present in the Priabonian (Bismouth & Bonnefous 1981; Tlig *et al.* 2010). The Lower Oligocene succession comprises nummulitic limestones but no coralgal assemblages (Salaj & van Houten 1988). During the Chattian, the deposition at the Tunisian carbonate platform was characterised by increasing continentalisation.

10) Libya (20°N)

Early Eocene deposits in the Libyan Sirte Basin are characterised by frequent nummulitic limestones (Ahlbrandt 2001). Tawadros (2001) reports on solitary corals in the uppermost Lutetian to Priabonian limestones. The first extended reefal limestones are recorded from the Early Oligocene (Abdulsamad & Barbieri 1999).

11) Egypt (20°N)

Carbonate platform successions in Egypt are dominated by larger benthic foraminifera limestones from the Early Eocene (Schuster 1996a, 1996b; Wielandt 1996; Hoentzsch *et al.* 2011a, 2011b). Rare isolated coral fragments from the Early Eocene are found in the Eastern Desert (Galala platform; Hoentzsch *et al.* 2011a, 2011b) and from the latest Lutetian in the Western Desert, whereas nummulitic limestones prevailed throughout the Eocene (Tawadros 2001). During the Oligocene, major carbonate platforms of the Egyptian shelf were subaerially exposed and destroyed.

The compiled records of Palaeogene circum-Tethyan platform associations reveal a significant trend regarding timing and latitudinal distribution of larger benthic foraminifera and hermatypic corals. Following the definition of circum-Tethyan platform stages of Scheibner and Speijer (2008a), we expand this classification from the Early Eocene to the Early Oligocene and redefine the stratigraphic range of platform stage III. We introduce 3 further circum-Tethyan platform stages characterised by a) the recovery of isolated coral faunas during the Bartonian in the northern Tethys (platform stage IV), the first larger reefal complexes at the northern Tethys and a recovery of the coral fauna in the southern Tethys during the Priabonian (platform stage V), and b) the Tethyan-wide coexistence of larger benthic foraminifera and coral faunas in the Oligocene (platform stage VI). Oligocene to Miocene latitudinal trends of Cenozoic reef patterns are illustrated in Perrin and Kiessling (2010).

5.1.1. Platform stage III (55.5–40.4 Ma; SBZ 5–16)

Platform stage III, introduced by Scheibner and Speijer (2008a) is defined by the occurrence of typical Eocene larger benthic foraminifera assemblages (Early Palaeogene chronofauna: *Nummulites* sp., *Alveolina* sp., *Assilina* sp., orthophragminids, *Orbitolites* sp.; Buxton & Pedley 1989; McGowran & Li 2001) and rare or absent hermatypic coral build-ups (Figures 6 and 7; 'Palaeogene gap' in coral abundance; Wilson & Rosen 1998). However, in several areas in the northern-temperate Tethyan realm (Northern Calcareous Alps, Pyrenees, and Maiella Platform), smaller coral patch reefs are recorded (Figure 6). The size and abundance of coral communities in those areas are significantly smaller than in the Palaeocene. Exceptional warm temperatures in higher latitudes caused the expansion of the tropical reef belt above 80°N (Kiessling 2001).

5.1.2. Platform stage IV (40.4–37.2 Ma; SBZ 17–18)

Platform stage IV represents a transitional stage between circum-Tethyan larger benthic foraminifera-dominated carbonate platforms during the Ypresian–Lutetian and the recovery of circum-Tethyan coral faunas during the Priabonian–Oligocene (Figures 6 and 7). The first larger Tethyan coral build-ups were recorded from the latest Lutetian (Perrin 2002). During the Bartonian, the occurrence of smaller patch reefs in overall larger benthic foraminifera-dominated platforms increased in the northern Tethyan realm (43°N to 30°N). In contrast to the recovery of the coral fauna in the northern temperate Tethys, the southern Tethyan realm remained coral-free.

5.1.3. Platform stage V (37.2–33.9 Ma; SBZ 19–20)

The global cooling event at the Bartonian–Priabonian boundary represents a major caesura in the evolution of Tethyan carbonate platform assemblages (Figures 1, 6, and 7). Many Early Eocene larger benthic foraminifera disappeared due to increasing trophic resources at the shelves (eutrophic Priabonian chronofauna; McGowran & Li 2001). Besides the demise of larger benthic foraminifera species, significantly lower temperatures during the Priabonian favoured the expansion of coral communities in the northern Tethys and led to the recovery of the coral fauna in the southern Tethys (Figures 6 and 7). Besides this latitudinal differentiation, increasing growth rates in coral reefs also varied between the Eastern and the Western Tethys. In the Western Tethys, increasing coral growth has been dated from the Late Eocene, whereas coral growth in the Eastern Tethys has not been described until the Early Eocene (Wood 1999). This observation is in contrast to the study of Kiessling (2001, 2002), who demonstrates a general slight constriction in coral reef growth during the Late Eocene and Early Oligocene. However, the specific diversity of corals increased significantly and all modern coral families appeared at the end of the Eocene (Wood 1999).

5.1.4. Platform stage VI (33.9–?; SBZ 21–?)

The base of platform stage VI coincides with the massive temperature drop related to the Oi-1 glaciation. This climatic caesura caused the extinction of orthophragminids and a strong decline in coral abundance but no extinction (Wood 1999). New larger benthic foraminifera emerged that were more tolerant to the cooler climate of the Late

Palaeogene. This Oligocene–Miocene larger benthic foraminifera chronofauna is dominated by lepidocyclinids, smaller nummulitids, and miogypsinids (Buxton & Pedley 1989; McGowran & Li 2001). Increasing oligotrophic conditions during the Early Oligocene favoured the proliferation of larger coral communities throughout the Tethys. However, the large-scale glacio-eustatic sea level fall, which coincided with the glaciation, caused the continuing continentalisation and destruction of many Tethyan carbonate shelves (Figures 6 and 7).

5.2. Variations in the evolution of larger benthic foraminifera and corals at the Prebetic platform

The Prebetic carbonate platform represents an exception in the evolution of the Eocene coral fauna in the northern Tethys. The first coral records are found in the Late Eocene, whereas carbonate platforms in comparable latitudes reveal the first frequent coral records during the Lutetian (Maiella Platform, Pyrenees) or Bartonian (North Adriatic Platform).

The causes for the absence of Middle Eocene coral faunas in the Prebetics are supposed to be related to repeated tectonic perturbations throughout the Palaeogene (Figures 1 and 4). Frequent phases of tectonic deformation in the hinterland as well as the continuing convergence of the Betic domain towards the Prebetic shelf led to a high environmental instability. Repeated uplift at the Iberian hinterland linked to a tropical humid to semi-humid climate caused the erosion and discharge of large amounts of terrigenous deposits toward the shelf (Postigo Mijarra *et al.* 2009). High-resolution carbon isotope records from the hemipelagic Relleu section indicate a depositional system that is strongly decoupled from the global carbon cycle (Figure 5). This decoupling is related to an increasing regional environmental impact in the Prebetic realm. Furthermore, the continuing convergence of the Betic domain may be related to an increasing isolation of the Prebetic shelf. A similar scenario has been described for the Early Eocene Egyptian shelf (Hoentzsch *et al.* 2011b). Tectonic uplift along the SE Mediterranean Syrian Arc-Fold Belt associated with the closure of the Eastern Tethyan seaway due to the initial contact between India and Eurasia led to an increasing restriction of the Egyptian Eastern Desert Intrashelf Basin (Hoentzsch *et al.* 2011b). Assemblages of coralline red algae, green algae, and larger benthic foraminifera indicate higher trophic resources in the Egyptian platform succession (Hallock & Schlager 1986; Vecsei 2003; Bassi 2005). A similar microfacies has been detected at the Palaeogene Prebetic succession. James *et al.* (1999) concluded that the combination of warm–temperate conditions and mesotrophic nutrient influx promotes coralline algae and bryozoan growth rather than the proliferation of reef-building corals. Recent studies have shown that increased terrestrial sediment influx decreases coral reef viability (Ryan *et al.* 2008). Copper (1994) links global coral reef crises in the Earth's history to periods of major tectonic reorganisation and climate change.

In contrast to the described scenario, enhanced nutrient availability and shelf restriction may not hinder the proliferation of corals. In the Pyrenees, Eocene non-framework coral build-ups have also developed in mesotrophic, turbid, and poorly illuminated environments with high terrestrial sediment discharge (Morsilli *et al.* 2012). Leinfelder (1997) demonstrated the occurrence of coral reefs in siliciclastic settings in the Late Jurassic of Portugal. Pleistocene and Holocene mixed siliciclastic-carbonate settings with coral proliferation are described from volcanoclastic-influenced shelves in Indonesia (Wilson & Lokier 2002).

The distribution of larger benthic foraminifera at the Prebetic platform is comparable to the general evolution of larger benthic foraminifera in the Tethys. The significant larger foraminifera turnover at the Palaeocene–Eocene boundary has been recorded for the first time in the Prebetic realm. Besides the prominent larger foraminifera turnover, subsequent specific transitions are more gradual than abrupt. Increasing records of larger benthic foraminifera are often related to tectonically driven mass wasting intervals (Figure 4). However, a prominent demise in the abundance of larger benthic foraminifera and the dominance of miliolids and soritids during the upper Lutetian and Bartonian indicates the tectonically driven restriction of the platform. The mass occurrence of *Solenomeris* sp. during the Priabonian has also been observed in the Early Eocene Pyrenean domain (Perrin 1992; Plaziat & Perrin 1992). The occurrence of *Solenomeris* build-ups is attributed to larger benthic foraminifera reef bodies that stretch for many kilometres. Furthermore, ecological similarities between *Solenomeris* and coral reefs probably indicate environmental similarities for both organism groups. However, *Solenomeris* is understood to tolerate more unfavourable conditions regarding light and trophic regime than corals. Plaziat and Perrin (1992) link the occurrence of *Solenomeris* to the northern limit of coral reef growth. In the Prebetics, the first coral records after the Palaeocene–Eocene Thermal Maximum are found in the Early Oligocene (Figure 4). The mass occurrence of *Solenomeris* during the Late Eocene probably represents a transitional stage in coral recovery in the study area.

5.3. Global vs. regional carbon isotope trends and the relation to Late Eocene–Oligocene platform evolution

The evolution of the global carbon cycle, expressed in the ratio of stable carbon isotopes ($\delta^{13}C$), is controlled by major carbon fluxes driven by volcanism, tectonics, the expansion of ice sheets, and changing Earth parameters. However, global signals are superimposed by regional

carbon fluxes, which are related to changes in sea level, productivity, and carbon burial, especially on marginal shelves.

Carbon isotope records based on bulk rock measurements indicate trends that are comparable to the high-resolution $\delta^{13}C$ records for deep marine benthic foraminifera compiled by Zachos *et al.* (2001) (Exmouth Plateau, Eastern Indian Ocean; Thomas *et al.* 1992). The carbon isotope ratios of deep marine bulk rock and benthic foraminifera reveal the evolution of the open ocean reservoir. However, the carbon isotopes of peri-platform deposits are strongly influenced by regional tectonic, oceanographic, and climatic conditions and may significantly vary from those of the open ocean.

Carbon isotope trends of marginal hemipelagic and pelagic sediments have been used as a proxy for Cenomanian–Turonian sea level fluctuations since the late 1980s. Arthur *et al.* (1987) suggested a relationship between sediment erosion and decreasing $\delta^{13}C$ in the geological record. A shift to increasingly negative $\delta^{13}C$ ratios requires the input of isotopically lighter carbon (^{12}C), by such means as the input of oxidised organic matter from sediments during sea level rises. This theoretical approach was proven by Hilbrecht *et al.* (1986), who revealed a coupling of sea level fluctuations and long-term carbon isotope trends in the Cenomanian and Turonian of NW Germany. Mitchell *et al.* (1996) and Voigt and Hilbrecht (1997) confirmed that the long-term enrichment in heavier carbon isotopes is strongly related to long-term eustatic sea level rise. Increases and positive maxima in $\delta^{13}C$ correspond to phases of sediment accumulation during sea level highstands and transgressions. A trend towards $\delta^{13}C$ depleted ratios and negative maxima in $\delta^{13}C$ correspond to phases of sediment erosion and reworking during sea level lowstands and regressions (Hilbrecht *et al.* 1986; Voigt & Hilbrecht 1997).

Swart (2008) demonstrated a strong relationship between Late Cenozoic sea level changes and the $\delta^{13}C$ trends in carbonate platform systems. Aragonite-producing organisms proliferate at carbonate platforms especially during transgressions and high sea levels. The chemical signature of aragonite reveals more positive $\delta^{13}C$ ratios than pelagic deposits without major aragonite concentrations. Following this concept, positive bulk rock $\delta^{13}C$ ratios indicate periods with a high sea level at carbonate platforms, whereas depleted bulk rock $\delta^{13}C$ ratios indicate periods with a low sea level. This relation is decoupled from the isotopic changes of the global carbon cycle. The impact of $\delta^{13}C$ enrichment during sea level highstands requires the presence of major aragonite-producing organisms (benthic green and red algae (except coralline), bivalves, gastropods, and serpulid worm tubes; according to Van de Poel & Schlager 1994; Lowenstam & Weiner 1989; Flügel 2004).

The Late Eocene–Early Oligocene carbon isotope evolution in the Prebetic realm reveals a prominent decoupling of the shelf from the global carbon cycle, especially during the latest Eocene and late Rupelian–early Chattian (Figure 4). The significant differences in the carbon isotope evolution are attributed to a strong regional impact on the Prebetic realm and are especially reflected in the prominent variations in carbon isotopes between turbiditic limestones and hemipelagic background marls.

The Relleu section reveals 5 intervals of frequent turbiditic limestone and debris flow deposition (MWI 1–4; Figure 5). Limestones in the Priabonian MWI 1 are significantly enriched in heavier carbon. Microfacies indicate the predominance of aragonitic coralline red algae and calcitic larger benthic foraminifera (Figure 4). Following the approach of Swart (2008), aragonitic organisms, which flourish during times of relatively high sea level, favour the production of ^{13}C-enriched carbon isotopes. Global sea level and regional sequence stratigraphic reconstructions point to a flooding of the Prebetic platform prior to the Eocene–Oligocene boundary (Figure 1; Geel 2000; Miller *et al.* 2005). The significant shift towards increasingly negative $\delta^{13}C$ ratios in the Early Oligocene is attributed to the massive glacio-eustatic sea level of the Oi-1 glaciation, which caused a demise of aragonite-producing organisms at the platform. However, microfacies from the Ibi and Relleu sections do not indicate a demise of red algae abundance during the Oligocene. The ^{13}C-enriched turbidites of the Late Eocene also indicate the negligible discharge of ^{12}C-enriched organic matter to the Prebetic shelf.

Early Oligocene turbidite intervals (MWI 2–4) are characterised by converging carbon isotope ratios towards those of the hemipelagic background marls but a continuing depletion in the carbon isotope ratios (Figure 4). This depletion is in contrast to the open ocean data of Thomas *et al.* (1992) and Zachos *et al.* (2001). We suggest an increasing restriction of the Prebetic shelf basin that is related to a continuing sea level drop during the Early Oligocene and the convergence of the Betic domain towards the Iberian Massif. Continuing convergence of both domains caused the contraction of the Prebetic shelf and the Subbetic basin. An increasing deposition of terrestrial deposits generally during the Early Oligocene low-stand sea level may have shifted the carbon isotope signature towards more negative ratios (Hoentzsch *et al.* 2011b).

6. Conclusions

The analysis of 10 Tethyan carbonate platform successions supported by high-resolution microfacies and geochemical data from the Prebetic platform in SE Spain reveals the

following results regarding the palaeoenvironmental evolution of circum-Tethyan shallow marine carbonate factories during the Palaeogene:

1) Palaeogene shallow marine benthic assemblages of the Prebetic carbonate platform have been subdivided into distinct intervals that are related to major climatic thresholds. Palaeocene platform deposits are characterised by dominant corals, coralline red algae, and smaller benthic foraminifera. Increasing temperatures and decreasing trophic resources caused the demise of the major coral and coralline red algae association during the Early and Middle Eocene and favoured the predominance of larger benthic foraminifera. Significant cooling and enhanced trophic resources during the Late Eocene and Oligocene favoured the recovery of corals and coralline red algae and caused major shifts in the larger benthic foraminifera assemblages at the Prebetic platform. However, frequent syndepositional tectonic activity throughout the Palaeogene caused no significant impact on the prevailing benthic assemblages.

2) The distribution of larger benthic foraminifera and corals at 10 Palaeogene circum-Tethyan carbonate platforms has been compared with the records of the Prebetic succession. Following the classification of the circum-Tethyan platform stages (Scheibner & Speijer 2008b), the dominance of corals and larger foraminifera is strongly controlled by climatic variations during the Early Palaeogene.

We reinterpret platform stage III and introduce 3 new stages (IV–VI) that demonstrate the biotic evolution of carbonate platforms subsequent to the Palaeocene–Eocene thermal maximum.

Stage III is characterised by the predominance of larger benthic foraminifera and rare or absent coral build-ups throughout the Tethys and ranges from the Palaeocene–Eocene thermal maximum to the Lutetian–Bartonian boundary (SBZ 5–16). During the subsequent platform stage IV (SBZ 17–18), carbonate platforms were dominated by larger benthic foraminifera but corals also proliferated in the northern temperate Tethys. This trend is linked to the increasing cooling of higher latitudes whereas tropical realms remained warm. The Bartonian–Priabonian boundary represents another major cooling event that coincided with the demise of many symbiont-bearing larger benthic foraminifera and the expansion of coral faunas in the tropical southern Tethys (platform stage V; SBZ 19–20). Platform stage V coincides with the exceptional highly eutrophic Priabonian chronofauna in larger benthic foraminifera evolution. The final step in the transition from greenhouse to icehouse conditions is represented by the Oi-glaciation at the Eocene–Oligocene boundary. This temperature drop favoured the proliferation of major coral build-ups throughout the Tethys and their coexistence with newly emerged larger benthic foraminifera (platform stage VI, SBZ 21–?).

3) Carbon isotope ratios from the Prebetic platform indicate an increasing decoupling of the Prebetic shelf from the global carbon cycle during the Oligocene. Strongly negative carbon isotope ratios suggest increasing carbon burial at the shelf related to the massive sea level drop at the Eocene–Oligocene boundary. Furthermore, the continuing convergence of the Betic domain and the Iberian Craton caused the restriction of the Prebetic shelf, which led to increasing terrestrial sediment discharge.

Acknowledgements

The authors would like to thank Ralf Bätzel and Karin Gesierich for the excellent preparation of the samples, as well as Brit Kockisch and Monika Segl for the determination of the geochemical parameters. We thank reviewers Ercan Özcan and İsmail Ömer Yılmaz and editor Aral Okay for their valuable comments, which improved the manuscript considerably. This project is funded by the German Science Foundation (DFG-KU 642/22-1).

References

Abdulsamad, E.O. & Barbieri, R. 1999. Foraminiferal distribution and palaeoecological interpretation of the Eocene-Miocene carbonates at Al Jabal al Akhdar (northeast Libya). *Journal of Micropalaeontology* **18**, 45–65.

Accordi, G., Carbone, F. & Pignatti, J.S. 1998. Depositional history of a Paleogene carbonate ramp (Western Cephalonia, Ionian Islands, Greece). *Geologica Romana* **34,** 131–205.

Adatte, T., Bolle, M.-P., Kaenel, E.D., Gawenda, P., Winkler, W. & Salis, K.V. 2000. Climatic evolution from Palaeocene to earliest Eocene inferred from clay-minerals: a transect from northern Spain (Zumaya) to southern (Spain, Tunisia) and southeastern Tethys margins (Israel, Negev). *In:* Schmitz, B., Sundquist, B. & Andreasson, F.P. (eds), *Early Paleogene Warm Climates and Biosphere Dynamics*. Geological Society, Sweden, GFF, Uppsala, 7–8.

Ahlbrandt, T.S. 2001. *The Sirte Basin Province of Libya – Sirte-Zelten Total Petroleum System*. US Geological Survey Bulletin 2202-F.

Alegret, L., Ortiz, S., Arenillas, I. & Molina, E. 2010. What happens when the ocean is overheated? The foraminiferal response across the Paleocene-Eocene thermal maximum at the Alamedilla section (Spain). *Geological Society of America Bulletin* **122,** 1616–1624.

Alegret, L., Ortiz, S., Orue-Etxebarria, X., Bernaola, G., Baceta, J.I., Monechi, S., Apellaniz, E. & Pujalte, V. 2009. The Paleocene–Eocene thermal maximum: new data on microfossil turnover at the Zumaia section, Spain. *Palaios* **24,** 318–328.

Alonso-Chaves, F.M., Soto, J.I., Orozco, M., Kilias, A.A. & Tranos, M.D. 2004. Tectonic evolution of the Betic Cordillera: an overview. *Bulletin of the Geological Society of Greece* **36,** 1598–1607.

Angori, E., Bernaola, G. & Monechi, S. 2007. Calcareous nannofossil assemblages and their response to the Paleocene–Eocene thermal maximum event at different latitudes: ODP Site 690 and Tethyan sections. *Geological Society of America Special Papers* **424**, 69–85.

Arthur, M.A., Schlanger, S.O. & Jenkyns, H.C. 1987. The Cenomanian-Turonian oceanic anoxic event, II. Palaeoceanographic controls on organic-matter production and preservation. *Geological Society, London, Special Publications* **26**, 401–420.

Barattolo, F., Bassi, D. & Romano, R. 2007. Upper Eocene larger foraminiferal–coralline algal facies from the Klokova Mountain (southern continental Greece). *Facies* **53,** 361–375.

Bassi, D. 1998. Coralline algal facies and their palaeoenvironments in the Late Eocene of Northern Italy (Calcare di Nago, Trento). *Facies* **39,** 179–202.

Bassi, D. 2005. Larger foraminiferal and coralline algal facies in an Upper Eocene storm-influenced, shallow-water carbonate platform (Colli Berici, north-eastern Italy). *Palaegeography, Palaeoclimatology, Palaeoecology* **226,** 17–35.

Beavington-Penney, S.J., Wright, V.P., & Racey, A. 2005. Sediment production and dispersal on foraminifera-dominated early Tertiary ramps: the Eocene El Garia Formation, Tunisia. *Sedimentology* **52**, 537–569.

Beerling, D.J. 2000. Increased terrestrial carbon storage across the Palaeocene-Eocene boundary. *Palaeogeography, Palaeoclimatology, Palaeoecology* **161,** 395–405.

Benjamini, C. 1981. Limestone and chalk transitions in the Eocene of the Western Negev, Israel. *In*: Neale, J.W. & Brasier, M.D. (eds) *Microfossils from Recent and Fossil Shelf Seas*. British Micropalaeontological Society, 205–213.

Benjamini, C. & Zilberman, E. 1979. Late Eocene coral reefs of the western Negev, Israel. *Israel Journal of Earth Sciences* **28**, 42–46.

Bijl, P.K., Houben, A.J.P., Schouten, S., Bohaty, S.M., Sluis, A., Reichart, G.J., Damste, J.S.S. & Brinkhuis, H. 2010. Transient Middle Eocene atmospheric CO_2 and temperature variations. *Science* **330,** 819–821.

Bismuth, H. & Bonnefous, J. 1981. The biostratigraphy of carbonate deposits of the middle and upper Eocene in northeastern off-shore Tunisia. *Palaeogeography, Palaeoclimatology, Palaeoecology* **36**, 191–211.

Blankenship, C.L. 1992. Structure and palaeogeography of the external Betic Cordillera, southern Spain. *Marine and Petroleum Geology* **9**, 257–264.

Bohaty, S.M. & Zachos, J.C. 2003. Significant Southern Ocean warming event in the late middle Eocene. *Geology* **31,** 1017–1020.

Bolle, M.P. & Adatte, T. 2001. Palaeocene-early Eocene climatic evolution in the Tethyan realm: clay mineral evidence. *Clay Minerals* **36,** 249–261.

Bosellini, F.R. & Pappazzoni, C.A. 2003. Palaeoecological significance of coral-encrusting foraminiferan associations: a case-study from the Upper Eocene of northern Italy. *Acta Palaeontologica Polonica* **48,** 279–292.

Bowen, G.J., Beerling, D.J., Koch, P.L., Zachos, J.C. & Quatilebaum, T. 2004. A humid climate state during the Palaeocene/Eocene thermal maximum. *Nature* **452,** 495–499.

Brasier, M.D. 1995. Fossil indicators of nutrient levels. 2: Evolution and extinction in relation to oligotrophy. *In*: Bosence, D.W.J. & Allison, P.A. (eds) *Marine Palaeoenvironmental Analysis from Fossils* Geological Society Special Publication **83**, 133–150.

Buxton, M.W.N. & Pedley, H.M. 1989. A standardized model for Tethyan Tertiary carbonate ramps. *Journal of the Geological Society, London* **146,** 746–748.

Cahuzac, B. & Poignant, A. 1997. Essai de biozonation de l'Oligo-Miocène dans les bassins européens à l'aide des grands foraminifèrés néritiques. *Bulletin de la Societe Geologique de France* **168**, 155–169.

Copper, P. 1994. Ancient reef ecosystem expansion and collapse. *Coral Reefs* **13,** 3–11.

Cosovic, V., Drobne, K. & Moro, A. 2004. Paleoenvironmental model for Eocene foraminiferal limestones of the Adriatic carbonate platform (Istrian Peninsula). *Facies* **50,** 61–75.

Cramer, B.S., Wright, J.D., Kent, D.V. & Aubrey, M.P. 2003. Orbital climate forcing of $d^{13}C$ excursions in the late Paleocene-early Eocene (chrons C24n–C25n). *Paleoceanography* **18,** No. 4, 1097, doi:10.1029/2003PA000909, 2003.

Daod, H. 2009. Carbonate microfacies analysis of Sinjar Formation from Qara Dagh Mountains, South-west of Sulaimani City, Kurdistan Region, Iraq. *World Academy of Science, Engineering and Technology* **58**, 752–762.

Darga, R. 1992. Geologie, Paläontologie and Palökologie der südostbayrischen unter-Priabonen (Ober-Eozän) Riffkalkvorkommen des Eisenrichtersteins bei Hallthurm (Nördlichen Kalkalpen) und des Kirchberg bei Neubeuern (Helvetikum). *Münchner Geowissenschaftliche Abhandlungen Reihe A*, **23**, 1–166.

De Ruig, M.J., Smit, J., Geel, T. & Kooi, H. 1991. Effects of the Pyrenean collision on the Paleocene stratigraphic evolution of the southern Iberian margin (southeast Spain). *Geological Society of America Bulletin* **103,** 1504–1512.

De Conto, R.M., Pollard, D., Wilson, P.A., Pälike, H., Lear, C.H. & Pagani, M. 2008. Thresholds for Cenozoic bipolar glaciation. *Nature* **455,** 652–657.

Doblas, M. & Oyarzun, R. 1990. The late Oligocene-Miocene opening of the North Balearic Sea (Valencia basin, western Mediterranean): a working hypothesis involving mantle upwelling and extensional detachment tectonics. *Marine Geology* **94**, 155–163.

Eichenseer, H. & Luterbacher, H. 1992. The marine Paleogene of the Tremp Region (NE Spain) – depositonal sequences, facies history, biostratigraphy and controlling factors. *Facies* **27,** 119–152.

Eldrett, J.S., Greenwood, D.R., Harding, I.C. & Huber, M. 2009. Increased seasonality through the Eocene to Oligocene transition in northern high latitudes. *Nature* **459,** 969–974.

Everts, A.J.W. 1991. Interpreting compositional variations of calciturbidites in relation to platform-stratigraphy: an example from the Paleogene of SE Spain. *Sedimentary Geology* **71,** 231–242.

Flügel, E. 2004. *Microfacies of Carbonate Rocks: Analysis, Interpretation and Application*. Springer, Berlin.

Fontboté, J. & Vera, J. 1983. Introduccion de la Cordillera Betica. *In*: Comba, J. (ed), *Geologia de España Vol. 2*. Instituto Geológico y Minero de España, Madrid, 205–218.

Galdeano, C.S.D. 2000. Evolution of Iberia during the Cenozoic with special emphasis on the formation of the Betic Cordillera and its relation with the western Mediterranean. *Ciencias da Terra* **14**, 9–24.

Garcia-Hernandez, M., Lopez-Garrido, A.C., Rivas, P., Sanz de Galdeano, C. & Vera, I.A. 1980. Mesozoic palaeogeographic evolution of the external zones of the Betic Cordillera. *Geologie en Mijnbouw* **59**, 155–168.

Gawenda, P., Winkler, W., Schmitz, B. & Adatte, T. 1999. Climate and bioproductivity control on carbonate turbidite sedimentation (Paleocene to earliest Eocene, Gulf of Biscay, Zumaia, Spain). *Journal of Sedimentary Research* **69,** 1253–1261.

Geel, T. 1996. Paleogene to Early Miocene sedimentary history of the Sierra Espuna (Malaguide complex, internal zone of the Betic Cordilleras, SE Spain), evidence for extra-Malaguide (Sardinian?) provenance of Oligocene conglomerates: paleogeographic implications. *Estudios Geologicos*, **52**, 211–230.

Geel, T. 2000. Recognition of stratigraphic sequences in carbonate platform and slope deposits: empirical models based on microfacies analysis of Palaeogene deposits in southeastern Spain. *Palaeogeography, Palaeoclimatology, Palaeoecology* **155,** 211–238.

Geel, T., Roep, T.B. & Van Hinte, J.E. 1998. Eocene tectono-sedimentary patterns in the Alicante Region (southeastern Spain). *In*: De Graciansky, P.C., Hardenbol, J., Jaquin, T. & Vail, P.R. (eds), *Mesozoic and Cenozoic Sequence Stratigraphy of European Basins.* SEPM Special Publication **60,** 289–302.

Gibbs, S.J., Bralower, T.J., Bown, P.R., Zachos, J.C. & Bybell, L.M. 2006. Shelf and open-ocean calcareous phytoplankton assemblages across the Paleocene–Eocene thermal maximum: implications for global productivity gradients. *Geology* **34,** 233–236.

Hallock, P. 2005. Global change and modern coral reefs: new opportunities to understand shallow-water carbonate depositional processes. *Sedimentary Geology* **175,** 19–33.

Hallock, P., Premoli Silva, I. & Boersma, A. 1991. Similarities between planktonic and larger foraminiferal evolutionary trends through Paleogene paleoceanographic changes. *Palaeogeography, Palaeoclimatology, Palaeoecology* **83,** 49–64.

Hallock, P. & Schlager, W. 1986. Nutrient excess and the demise of coral reefs and carbonate platforms. *Palaios* **1,** 389–398.

Harzhauser, M. 2004. Oligocene gastropod faunas of the Eastern Mediterranean (Mesohellenic Trough/Greece and Esfahan–Sirjan Basin/Central Iran). *Courier Forschungsinstitut Senckenberg* **248**, 93–181.

Hilbrecht, H., Arthur, M. & Schlanger, S. 1986. The Cenomanian–Turonian boundary event: sedimentary, faunal and geochemical criteria developed from stratigraphic studies in NW-Germany, *In*: Walliser, O (ed), *Global Bio-Events: A Critical Approach Proceedings of the First International Meeting of the IGCP Project 216: "Global Biological Events in Earth History"*. Springer, Berlin, 345–351.

Hoentzsch, S., Scheibner, C., Kuss, H.J., Marzouk, A.M., & Rasser, M.W. 2011a. Tectonically driven ramp evolution at the southern margin of the Tethys – the Lower to Middle Eocene succession of the Galala Mountains, Egypt. *Facies*. **57,** 51–72.

Hoentzsch, S., Scheibner, C., Guasti, E., Kuss, J., Marzouk, A.M. & Rasser, M. 2011b. Increasing restriction of the Egyptian shelf during the Early Eocene? – New insights from a southern Tethyan carbonate platform. *Palaegeography, Palaeoclimatology, Palaeoecology* **302,** 349–366.

Hottinger, L. 1997. Doktor Honoris Causa Lukas Hottinger.

Hottinger, L. 1998. Shallow benthic foraminifera at the Paleocene–Eocene boundary. *Strata, Serie 1* **9,** 61–64.

Hottinger, L. 2001. Learning from the past? *In*: Box, E. & Pignatti, S. (eds), *Volume IV: The Living World. Part Two.* Academic Press, San Diego, USA, 449–477.

İslamoğlu, Y., Harzhauser, M., Gross, M., Jiménez-Moreno, G., Coric, S., Kroh, A., Rögl, F. & van der Made, J. 2010. From Tethys to Eastern Paratethys: Oligocene depositional environments, paleoecology and paleobiogeography of the Thrace Basin (NW Turkey). *International Journal of Earth Sciences* **99**, 183–200.

Ivany, L.C., Patterson, W.P. & Lohmann, K.C. 2000. Cooler winters as a possible cause of mass extinctions at the Eocene/Oligocene boundary. *Nature* **407**, 887–890.

James, N.P., Collins, L.B., Bone, Y. & Hallock, P. 1999. Subtropical carbonates in a temperate realm: modern sediments on the Southwest Australian shelf. *Journal of Sedimentary Research* **69**, 1297–1321.

Jovane, L., Florindo, F., Coccioni, R., Dinares-Turell, J., Marsili, A., Monechi, S., Roberts, A.P. & Sprovieri, M. 2007. The middle Eocene climatic optimum event in the Contessa highway section, Umbrian Apennines, Italy. *Geological Society of America Bulletin* **119,** 413–427.

Kemper, E. 1966. Beobachtungen an obereozänen Riffen am Nordrand des Ergene-Beckens (Türkisch–Thrazien). *Neues Jahrbuch für Geologie und Paläontologie, Abhandlungen* **125**, 540–554.

Kennett, J. & Stott, L. 1991. Abrupt deep-sea warming, palaeoceanographic changes and benthic extinctions at the end of the Palaeocene. *Nature* **53**, 225–229.

Kenter, J.A.M., Reymer, J.J.G. & Van der Straten, H.C. 1990. Facies patterns and subsidence history of the Jumilla-Cieza region (southeastern Spain). *Sedimentary Geology* **67,** 263–280.

Kiessling, W. 2001. Paleoclimatic significance of Phanerozoic reefs. *Geology* **29,** 751–754.

Kiessling, W. 2002. Secular variations in the Phanerozoic reef ecosystem. *In*: Kiessling, W., Flügel, E. & Golonka, J. (eds), *Phanerozoic Reef Patterns.* SEPM Special Publication **72,** 625–690.

Krasheninnikov, V.A. 2005. Part II – Syria – Paleogene. *In*: Krasheninnikov, V.A., Hall, J.K., Hirsch, F., Benjamini, C. & Flexer, A. (eds), *Geological Framework of the Levant. Volume I: Cyprus and Syria.* Historical Productions-Hall, Jerusalem, 299–342.

Leinfelder, R.R. 1997. Coral reefs and carbonate platforms within a siliciclastic setting: general aspects and examples from the Late Jurassic of Portugal. *Proceedings of the 8th International Coral Reef Symposium* **2**, 1737–1742.

Less, G., Özcan, E., Papazzoni, C.A. & Stockar, R. 2008. The middle to late Eocene evolution of nummulitid foraminifer Heterostegina in the Western Tethys. *Acta Palaeontologica Polonica* **53**. 317–350.

Less, G., Özcan, E., & Okay, A.I. 2011. Stratigraphy and larger foraminifera of the Middle Eocene to Lower Oligocene shallow-marine units in the northern and eastern parts of the Thrace Basin, NW Turkey. *Turkish Journal of Earth Sciences* **20**, 793–845.

Less, G., & Özcan, E. 2012. Bartonian–Priabonian larger benthic foraminiferal events in the western Tethys. *Austrian Journal of Earth Sciences* **105**, 129–140.

Lopez-Martinez, N. 1989. Tendencias en plaeobiogeografia el futuro de la biogeografia del pasado *In*: Aguirre, E. (ed), *Paleontologia*, CSIC, Madrid, 271–299.

Louks, R.G., Moody, R.T.J., Bellis, J.K. & Brown, A.A. 1998. Regional depositional setting and pore network systems of the El Garia Formation (Metlaoui Group, Lower Eocene), offshore Tunisia. *In*: MacGregor, D.S., Moody, R.T.J. & Clark-Lowes, D.D. (eds), *Petroleum Geology of North Africa.* Geological Society, London, Special Publication **132**, 355–374.

Lourens, L.J., Sluijs, A., Kroon, D., Zachos, J.C., Thomas, E., Röhl, U., Bowles, J. & Raffi, I. 2005. Astronomical pacing of late Palaeocene to early Eocene global warming events. *Nature* **435,** 1083–1087.

Lowenstam, H.A. & Weiner, S. 1989. *On Biomineralization*. Oxford University Press, New York.

Martin-Chivelet, J. & Chacon, B. 2007. Event stratigraphy of the upper Cretaceous to lower Eocene hemipelagic sequences of the Prebetic Zone (SE Spain): record of the onset of tectonic convergence in a passive continental margin. *Sedimentary Geology* **197,** 141–163.

Martinez del Omo, W. 2003. La Plataforma Cretácica del Prebético y su falta de continuidad por el Margen Sudibérico. *Cuadernos de Geología Ibérica, Volumen especial, Nuevas perspectivas sobre el Cretácico de España* **29**, 111–133.

McGowran, B. 2009. The Australo-Antarctic Gulf and the Auversian facies shift. *Geological Society of America Special Papers* **452**, 215–240.

McGowran, B. & Li, Q. 2000. Evolutionary palaeoecology of Cainozoic foraminifera: Tethys, Indo-Pacific, Southern Australasia. *Historical Biology* **15,** 3–27.

Meulenkamp, J.E. & Sissingh, W. 2000. Early to Middle Ypresian, late Lutetian, late Rupelian, early Burdigalian, early Langhian, late Tortonian, Piacenzian/Gelasian, *In*: Dercourt, J. & Gaetani, M., et al. (eds), *Atlas Peri-Tethys, Palaeogeographical Maps*. CCGM/CGMW, Paris, 17–23.

Meulenkamp, J.E. & Sissingh, W. 2003. Tertiary palaeogeography and tectonostratigraphic evolution of the northern and southern Peri-Tethys platforms and the intermediate domains of the African-Eurasian convergent plate boundary zone. *Palaeogeography, Palaeoclimatology, Palaeoecology* **196,** 209–228.

Miller, K.G., Kominz, M.A., Browning, J.V., Wright, J.D., Mountain, G.S., Katz, M.E., Sugarman, P.J., Cramer, B.S., Christie-Blick, N. & Pekar, S.F. 2005. The Phanerozoic record of global sea-level change. *Science* **310,** 1293–1298.

Mitchell, S.F., Paul, C.R.C. & Gale, A.S. 1996. Carbon isotopes and sequence stratigraphy. *Geological Society, London, Special Publications* **104**, 11–24.

Molina, E., Angori, E., Arenillas, I., Monechi, S. & Schmitz, B. 2000. Integrated stratigraphy across the Paleocene/Eocene boundary at Campo, Spain. *GFF* **122,** 106–107.

Monechi, S. & Tori, F. 2010. Calcareous nannoplankton changes during the middle Eocene in the Agost section (Spain): evidence for hyperthermal events. *American Geophysical Union Fall Meeting 2010, San Francisco, Abstracts.*

Morsilli, M., Bosellini, F.R., Pomar, L., Hallock, P., Aurell, M. & Papazzoni, C.A. 2012. Mesophotic coral buildups in a prodelta setting (Late Eocene, southern Pyrenees, Spain): a mixed carbonate-siliciclastic system. *Sedimentology* **59,** 766–794.

Moussavian, E. & Vecsei, A. 1995. Paleocene reef sediments from the Maiella carbonate platform, Italy. *Facies* **32,** 213–222.

Nebelsick, J., Rasser, M. & Bassi, D., 2005. Facies dynamics in Eocene to Oligocene circumalpine carbonates. *Facies* **51**, 197–217.

Ortiz, S., Gonzalvo, C., Molina, E., Rodriguez-Tovar, F.J., Uchman, A., Vanderberghe, N. & Zeelmaekers, E. 2008. Palaeoenvironmental turnover across the Ypresian–Lutetian transition at the Agost section, Southeastern Spain: in search of a marker event to define the stratotype for the base of the Lutetian Stage. *Marine Micropaleontology* **69,** 297–313.

Orue-Etxebarria, X., Pujalte, V., Bernaolo, G., Apellaniz, E., Baceta, J.I., Payros, A., Nunez-Betelu, K., Serra-Kiel, J. & Tosquella, J. 2001. Did the Late Paleocene thermal maximum affect the evolution of larger foraminifers? Evidence from calcareous plankton of the Campo Section (Pyrenees, Spain). *Marine Micropaleontology* **41,** 45–71.

Özcan, E., Less, G., Okay, A.I., Baldi-Beke, M., Kollanyi, K., & Yılmaz, Ö. 2010. Stratigraphy and larger foraminifera of the Eocene shallow-marine and olistostromal units of the southern part of the Thrace Basin, NW Turkey. *Turkish Journal of Earth Sciences*. **19**, 27–77.

Özcan, E., Less, G., Báldi-Beke, M., & Kollányi, K. 2010a. Oligocene hyaline larger foraminifera from Keleresdere Section (Mus, Eastern Turkey). *Micropaleontology*. **56**, 465–493.

Payros, A., Pujalte, V., Tosquella, J. & Orue-Etxebarria, X. 2010. The Eocene storm-dominated foralgal ramp of the western Pyrenees (Urbasa–Andia Formation): An analogue of future shallow-marine carbonate systems? *Sedimentary Geology* **228,** 184–204.

Pearson, P.N., Van Dongen, B.E., Nicholas, C.J., Pancost, R.D., Schouten, S., Singano, J.M. & Wade, B.S. 2007. Stable warm tropical climate through the Eocene Epoch. *Geology* **35,** 211–214.

Perrin, C. 1992. Signification Écologique des foraminifères acervulinidés et leur role dans la formation de faciès récifaux et organogènes depuis le Paléocène. *Geobios* **25,** 725–751.

Perrin, C. 2002. Tertiary: The emergence of modern reef ecosystems. *In*: Kiessling, W., Flügel, E. & Golonka, J. (eds), *Phanerozoic Reef Patterns,* SEPM Special Publication **72,** 587–621.

Perrin, C. & Kiessling, W. 2010. Latitudinal trends in Cenozoic reef patterns and their relationship to climate. *In*: Mutti, M., Piller, W. & Betzler, C. (eds), *Carbonate systems during the Oligocene–Miocene climatic transition.* Wiley-Blackwell, 17–33.

Plaziat, J.C. & Perrin, C. 1992. Multikilometer-sized reefs built by foraminifera (Solenomeris) from the early Eocene of the Pyrenean domain (S. France, N. Spain): palaeoecologic relations with coral reefs. *Palaeogeography, Palaeoclimatology, Palaeoecology* **96,** 195–231.

Postigo Mijarra, J.M., Barrón, E., Gómez Manzaneque, F. & Morla, C. 2009. Floristic changes in the Iberian Peninsula and Balearic Islands (south-west Europe) during the Cenozoic. *Journal of Biogeography* **36**, 2025–2043.

Prothero, D.R. 2003. Chronostratigraphy of the Pacific Coast marine Eocene-Oligocene transition. *In:* Prothero, D.R., Ivany, L.C. & Nesbitt, E.A. (eds), *From Greenhouse to Icehouse: The Marine Eocene–Oligocene Transition.* Columbia University Press, New York, 1–12.

Rasser, M. 1994. Facies and palaeoecology of rhodoliths and acervulinid macroids in the Eocene of the Krappfeld (Austria). *Beiträge zur Paläontologie* **19,** 191–217.

Rasser, M.W. & Piller, W.E. 2004. Crustose algal frameworks from the Eocene Alpine Foreland. *Palaeogeography, Palaeoclimatology, Palaeoecology* **206,** 21–39.

Ryan, K.E., Walsh, J.P., Corbett, D.R. & Winter, A. 2008. A record of recent change in terrestrial sedimentation in a coral-reef environment, La Parguera, Puerto Rico: a response to coastal development? *Marine Pollution Bulletin* **56**, 1177–1183.

Salaj, J.B. & Van Houten, F. 1988. Cenozoic palaeogeographic development of northern Tunisia, with special reference to the stratigraphic record in the Miocene trough. *Palaeogeography, Palaeoclimatology, Palaeoecology* **64**, 43–57.

Scheibner, C., Speijer, R.P. & Marzouk, A.M. 2005. Larger foraminiferal turnover during the Paleocene/Eocene thermal maximum and paleoclimatic control on the evolution of platform ecosystems. *Geology* **33,** 493–496.

Scheibner, C., Rasser, M.W. & Mutti, M. 2007. Facies changes across the Paleocene–Eocene boundary: The Campo section (Pyrenees, Spain) revisited. *Palaeogeography, Palaeoclimatology, Palaeoecology* **248,** 145–168.

Scheibner, C. & Speijer, R.P. 2008a. Decline of coral reefs during late Paleocene to early Eocene global warming. *Earth* **3,** 19–26.

Scheibner, C. & Speijer, R.P. 2008b. Late Paleocene–early Eocene Tethyan carbonate platform evolution – A response to long- and short-term paleoclimatic change. *Earth-Science Reviews* **90,** 71–102.

Schmitz, B., Pujalte, V. & Nunez-Betelu, K. 2001. Climate and sea-level perturbations during the initial Eocene thermal maximum: evidence from siliciclastic units in the Basque Basin (Emua, Zumaia and Trabakua Pass), northern Spain. *Palaeogeography, Palaeoclimatology, Palaeoecology* **165,** 299–320.

Schmitz, B. & Pujalte, V. 2003. Sea-level, humidity, and land-erosion records across the initial Eocene thermal maximum from a continental-marine transect in northern Spain. *Geology* **31,** 689–692.

Schuster, F. 1996. Paleoecology of Paleocene and Eocene corals from the Kharga and Farafra Oases (Western Desert, Egypt) and the depositional history of the Paleocene Abu Tartur carbonate platform, Kharga Oasis. *Tübinger Geowissenschaftliche Arbeiten* **A31,** 1–96.

Schuster, F. 1996a. Paleocene coral reefs and related facies associations, Kharga Oasis, Western Desert, Egypt. *In*: Reitner, J., Neuweiler, F. & Gunkel, F. (eds), *Global and Regional Controls on Biogenic Sedimentation. I Reef Evolution,* Göttinger Arbeiten zur Geologie und Paläontologie, **Sb2,** 169–174.

Schuster, F. 2002. Scleractinian corals from the Oligocene of the Qom formation (Esfahan–Sirjan fore-arc basin, Iran). *Courier Forschungsinstitut Senckenberg* **239**, 5–55.

Seilacher, A. 1967. Bathymetry of trace fossils. *Marine Geology* **5**, 413–428.

Serra-Kiel, J., Hottinger, L., Caus, E., Drobne, K., Ferrandez, C., Jauhri, A.K., Less, G., Pavlovec, R., Pignatti, J., Samso, J.M., Schaub, H., Sirel, E., Strougo, A., Tambareau, Y., Tosquella, J. & Zakrevskaya, E. 1998. Larger foraminiferal biostratigraphy of the Tethyan Paleocene and Eocene. *Bulletin de la Société Géologique de France* **169,** 281–299.

Swart, P.K. 2008. Global synchronous changes in the carbon isotopic composition of carbonate sediments unrelated to changes in the global carbon cycle. *Proceedings of the National Academy of Sciences* **105**, 13741–13745.

Taktak, F., Kharbachi, S., Bouaziz, S. & Tlig, S. 2010. Basin dynamics and petroleum potential of the Eocene series in the gulf of Gabes, Tunisia. *Journal of Petroleum Science and Engineering* **75**, 114–128.

Tawadros, E.E. 2001. *The Geology of Egypt and Libya*. Balkema, Rotterdam.

Thomas, E., Shackleton, N. & Hall, M. 1992. Data report: carbon isotope stratigraphy of Paleogene bulk sediments, Hole 762C (Exmouth Plateau, eastern Indian Ocean), in: Von Rad, U., Haq, B.U. et al. (eds), Proceedings ODP, Scientific Results. Ocean Drilling Program, College Station, TX, 897–901.

Thomas, E. & Zachos, J.C. 2000. Was the late Paleocene thermal maximum a unique event? *GFF* **122,** 169–170.

Thomas, M.F.H., Bodin, S., Redfern, J. & Irving, D.H.B. 2010. A constrained African craton source for the Cenozoic Numidian Flysch: implications for the palaeogeography of the western Mediterranean basin. *Earth-Science Reviews* **101**, 1–23.

Tlig, S., Sahli, S., Er-Raioui, L., Alouani, R. & Mzoughi, M. 2010. Depositional environment controls on petroleum potential of the Eocene in the north of Tunisia. *Journal of Petroleum Science and Engineering* **71,** 91–105.

Van de Poel, H.M. & Schlager, W. 1994. Variations in Mesozoic–Cenozoic skeletal mineralogy. *Geologie & Mijnbouw* **74**, 31–51.

Vecsei, A. 2003. Nutrient control of the global occurrence of isolated carbonate banks. *International Journal of Earth Sciences* **92,** 476–481.

Vecsei, A. & Moussavian, E. 1997. Paleocene reefs on the Maiella platform margin, Italy: an example of the effects of the Cretaceous/Tertiary boundary events on reefs and carbonate platforms. *Facies* **36,** 123–140.

Vecsei, A. & Sanders, D.G.K. 1997. Sea-level highstand and lowstand shedding related to shelf margin aggradation and emersion, Upper Eocene–Oligocene of Maiella carbonate platform, Italy. *Sedimentary Geology* **112,** 219–234.

Vergés, J., Fernàndez, M. & Martìnez, A. 2002. The Pyrenean orogen: pre-, syn-, and post-collisional evolution. *In*: Rosenbaum, G. & Lister, G. (eds), *Reconstruction of the Evolution of the Alpine-Himalayan Orogen*. Journal of the Virtual Explorer **8**, 55–74.

Voigt, S. & Hilbrecht, H. 1997. Late Cretaceous carbon isotope stratigraphy in Europe: correlation and relations with sea level and sediment stability. *Palaeogeography, Palaeoclimatology, Palaeoecology* **134**, 39–59.

Watts, A.B., Piatt, J.P. & Buhl, P. 1993. Tectonic evolution of the Alboran Sea basin. *Basin Research* **5**, 153–177.

Wei, W. 2004. Opening of the Australia–Antarctica Gateway as dated by nannofossils. *Marine Micropaleontology* **52**, 133–152.

Wielandt, U. 1996. Benthic foraminiferal paleoecology and microfacies investigations of Paleogene sediments from the Farafra Oasis, Western Desert, Egypt. *Tübinger Mikropaläontologische Mitteilungen* **13**, 1–78.

Wilson, M.E.J. & Lokier, S.W. 2002. Siliciclastic and volcaniclastic influences on equatorial carbonates: insights from the Neogene of Indonesia. *Sedimentology* **49,** 583–601.

Wilson, M.E.J. & Rosen, B.R. 1998. Implications of paucity of corals in the Paleogene of SE Asia: plate tectonics or centre of origin. *In*: Hall, R. & Holloway, J.D. (eds), *Biogeography and Geological Evolution of SE Asia.* Backhuys Publishers, Leiden, 165–195.

Wood, R. 1999. *Reef Evolution*. Oxford University Press.

Zachos, J., Pagani, M., Sloan, L., Thomas, E. & Billups, K. 2001. Trends, rhythms, and aberrations in global climate 65 Ma to present. *Science* **292,** 686–693.

Zachos, J.C., Dickens, G.R. & Zeebe, R.E. 2008. An early Cenozoic perspective on greenhouse warming and carbon-cycle dynamics. *Nature* **451,** 279–283.

Zamagni, J., Mutti, M. & Kosir, A. 2008. Evolution of shallow benthic communities during the Late Paleocene–earliest Eocene transition in the Northern Tethys (SW Slovenia). *Facies* **54,** 25–43.

Zanazzi, A., Kohn, M.J., MacFadden, B.J. & Terry, D.O. 2007. Large temperature drop across the Eocene–Oligocene transition in central North America. *Nature* **445**, 639–642.

Ziegler, M. 2001. Late Permian to Holocene paleofacies evolution of the Arabian Plate and its hydrocarbon occurrences. *GeoArabia* **6**, 445–505.

Ziegler, P.A. 1992. *Geological Atlas of Western and Central Europe* (2nd ed). Geological Society of London, London.